

# Hierarchical Framework for Space Exploration Campaign Schedule Optimization\*

Nicholas Gollins<sup>†</sup> and Koki Ho<sup>‡</sup>  
*Georgia Institute of Technology, Atlanta, Georgia, 30332*

Space exploration plans are becoming increasingly complex as public agencies and private companies target deep-space locations, such as cislunar space and beyond, which require long-duration missions and many supporting systems and payloads. Optimizing multi-mission exploration campaigns is challenging due to the large number of required launches as well as their sequencing and compatibility requirements, making the conventional space logistics formulations not scalable. To tackle this challenge, this paper proposes an alternative approach that leverages a two-level hierarchical optimization algorithm: a genetic algorithm is used to explore the campaign scheduling solution space, and each of the solutions is then evaluated using a time-expanded multi-commodity flow mixed-integer linear program. A number of case studies, focusing on the Artemis lunar exploration program, demonstrate how the method can be used to analyze potential campaign architectures. The method enables a potential mission planner to study the sensitivity of a campaign to program-level parameters such as logistics vehicle availability and performance, payload launch windows, and in-situ resource utilization infrastructure efficiency.

## Nomenclature

$c$	=	Crew consumables consumption rate (kg per crew member per day)
$C$	=	Mixed-integer linear program objective function cost multiplier
$C$	=	Set of co-payloads
$d$	=	Demand matrix
$\mathcal{D}$	=	Spacecraft domain
$\mathcal{E}$	=	Boolean variable defining whether an arc exists.
$f$	=	Objective function of commodity flow mixed-integer linear program

---

\*A previous version of this paper was presented at the AIAA SciTech Forum in National Harbor, MD & Virtual on January 23-27, 2023 (AIAA 2023-1965).

<sup>†</sup>PhD Candidate, Daniel Guggenheim School of Aerospace Engineering, AIAA Student Member.

<sup>‡</sup>Dutton-Duocoffe Professor, Associate Professor, Daniel Guggenheim School of Aerospace Engineering, AIAA Senior Member. kok-iho@gatech.edu

$\mathcal{F}$	=	Objective function of metaheuristic optimizer and output value of mixed-integer linear program commodity flow function
$i$	=	Origin node
$I$	=	Total number of logistics network nodes
$io$	=	Flow direction (in-to- or out-of-arc)
$I_{sp}$	=	Specific impulse (s)
$j$	=	Target node
$k$	=	Penalty function scaling coefficient
$m$	=	Quantity or mass (kg)
$m_{dry}$	=	Dry Mass (kg)
$m_{crew}$	=	Mass per Crew Member (kg per person)
$m_{pay}$	=	Payload capacity (kg)
$m_{prop}$	=	Propellant capacity (kg)
$n$	=	vehicle index
$N$	=	Total number of vehicle designs
$\mathcal{N}$	=	Number of duplicated time steps in the nonlinear penalty case study
$p$	=	Payload type index
$P$	=	Total number of commodity types
$P_F$	=	Number of float (continuous) commodity types
$P_I$	=	Number of integer commodity types
$\mathcal{P}$	=	Set of soft precursor payloads
$\mathcal{Q}$	=	Set of strict precursors payloads
$\mathcal{R}$	=	Set of programmatic requirements
$\mathcal{S}$	=	Set of vehicles that can form a stack
$\mathcal{S}'$	=	Set of stacks to which a vehicle belongs
$t$	=	Time index
$t_F$	=	Minimum time between launches (months)
$t_L$	=	Lower bound of launch window
$t_U$	=	Upper bound of launch window
$T_{LP}$	=	Total number of time steps in the linear program
$x$	=	Commodity flow (decision variable of mixed-integer linear program function)
$\mathbf{x}$	=	Metaheuristic decision vector and input variable to $\mathcal{F}$
$Z$	=	Propellant mass fraction

$\beta$	=	Propellant boil-off rate (% per day)
$\Gamma$	=	Metaheuristic cost function
$\Lambda$	=	Metaheuristic penalty function
$\phi$	=	Propellant oxidizer mass ratio
$\mu$	=	in-situ resource utilization maintenance supply requirement (kg per kg ISRU infrastructure per day)
$\rho$	=	in-situ resource utilization propellant production rate (kg propellant per kg in-situ resource utilization infrastructure per day)
$\tau$	=	Time of flight

## I. Introduction

THE Global Exploration Roadmap (GER), published by the International Space Exploration Coordination Group (ISECG) [1], lays out the development of a sustained crewed presence in beyond-low Earth orbit (LEO) locations over the coming decades. The document focuses particularly on lunar surface exploration and the planned Artemis program and supporting missions. Ref. [1] shows a possible sequence of missions in the Artemis and supporting programs, demonstrating the increasing cadence of missions launched to cislunar space over the coming decade. Historically, however, the crewed exploration of space has taken one of two forms:

- Early LEO missions, through the Apollo era, and the early Shuttle era, largely consisted of single-shot missions that carried all of the required material in a single launch.
- The International Space Station (ISS) era required a more sophisticated logistics plan, with a variety of resources sourced from different providers being delivered to the space station.

The plans laid out in the GER combine the challenges of deep-space exploration of the Apollo era with the complex logistics requirements of the ISS. This combination of increasing complexity and cadence of missions, many of which are interdependent, manufactures a necessity for efficient planning. It would be useful, therefore, for a would-be campaign architect to be able to find an optimal campaign plan for a particular set of programmatic and system assumptions, and to be able to study how the optimal plan reacts to changes in those assumptions. The optimization method presented in this paper is intended to serve as a process by which to obtain a well-performing baseline campaign plan according to pre-determined requirements.

There have been various studies in the space logistics research area to tackle such challenges. Network-based optimization, along with mixed-integer linear programming (MILP), was used to model ISS resource and traffic management and used to assess the usefulness of logistics vehicle designs [2, 3]. More recently, the field has expanded to address the problems of modern space systems optimization problems. Taylor *et al* [4] developed a MILP-based heuristic commodity flow model for interplanetary transport, in which commodity flow paths are pre-determined and then assigned to logistics vehicles. Later, the SpaceNet space logistics modeling framework utilized time-expanded

networks and was used to study ISS, lunar, and interplanetary logistics [5, 6]. More recently, multi-commodity flow models have been developed to calculate the optimal flow of spacecraft, payloads, and propellant through space [7, 8]. Furthermore, space logistics models have been developed further to incorporate spacecraft design into the overall mission optimization framework [9–12]. In practice, uncertainty can arise in many aspects of space mission planning. For example, Blossey [13] constructed a stochastic MILP to tackle commodity demand uncertainty in Mars mission planning. Other examples of sources of uncertainty could result from launch delay, in-space maneuver error, operational risks, and/or system failures. Chen *et al* established a method for adjusting an optimal commodity flow, for a given schedule, for robustness to launch delays [14].

While most of the existing space logistics mission design studies assumed a relatively well-defined set of requirements and hypothetical/simplified vehicles, in practice, space mission designers need to explore a large design space with a set of requirements that are not necessarily precisely defined and yet interdependent. For example, a multi-mission campaign needs to be scheduled with large possible launch windows while satisfying the payload delivery sequencing requirements and availability of each potential vehicle. Considering the large number of payloads that can feature in multi-mission exploration campaigns, there can be many combinations of choices of launch times for each payload within their respective launch windows, each with many choices of available vehicles. Different combinations can result in different logistics solutions, some more efficient than others. For smaller campaigns, an obvious solution might be, for example, to group all payloads into a single, larger spacecraft as a “ride-share” mission. However, the more payloads and possible vehicles that are involved in the campaign, the more difficult it becomes to navigate the solution space efficiently. This is due to the complex combinations of programmatic requirements and vehicle availability constraints creating a sparse solution space. It would be beneficial, therefore, to have a method by which to efficiently assess commodity flow parameters and model structures, such as launch schedules or vehicle properties.

While some of these complexity challenges have been tackled by MILP in conventional studies, these methods have significant limitations in terms of their scalability to the mission sequencing requirements and the number/types of payloads/vehicles. For example, the lower and upper bounds of payload launch times and vehicle availability can be translated into supply/demand times within the commodity flow in the conventional MILP formulation. However, more complex types of constraints such as payload or mission sequencing (e.g. payload X must launch before payload Y) place constraints on the interactions between the commodities within the MILP. This can be handled in the MILP by treating each individual payload as a separately-indexed commodity type, and tailoring sequencing constraints to each of those commodities, but creating more commodity types increases the size of the problem, and solving times can grow rapidly or the solver can encounter memory limitations. \* While other approaches exist by introducing auxiliary variables to enforce mission sequencing [15], those approaches still increase the numbers of (integer) variables and constraints and thus complexity. In addition to this, the solution space is sparse: a large number of infeasible solutions

---

\*The scalability issues of MILP are discussed further in Appendix A.

can lie between two feasible ones, which poses challenges to the solver.

Another drawback of using MILP is that it cannot capture a nonlinear cost function in commodity flow modeling. Methods exist for solving commodity flow problems with nonlinear costs appearing in the objective function [16] and/or with nonlinear constraints [17, 18]. However, these methods only work with continuous variables - mixed-integer nonlinear commodity flows are much more difficult to solve, but it is possible using metaheuristic algorithms [19]. Mixed-integer formulations are necessary in space logistics models due to the need to model the transport of discrete commodities such as spacecraft and crew.

To tackle the above challenges, this work aims to propose a generalized schedule optimization by using a multi-level optimization. Namely, a genetic optimization algorithm is used to explore scheduling solutions, which are evaluated using a logistics MILP formulation. Metaheuristic optimization has been utilized in previous space logistics works. Taylor *et al* used a heuristic random search algorithm to navigate solution to a commodity flow problem [4]; Chen and Ho [9] used simulated annealing optimization to integrate vehicle design with commodity flow; and Jagannatha and Ho [20] used a multi-objective genetic algorithm to find optimal parameters for in-space propellant depot supply chain design. In this work, the intended use of the genetic scheduling algorithm is to schedule the demand times of program payloads such as crew, habitats, rovers, or scientific equipment, for example, considering nonlinear constraints. At the same time, the MILP handles the "supporting" payloads such as crew supplies and maintenance equipment. This limits the number of payload-type indices required and therefore keeps the scale of the MILP problem manageable. An advantage of using a metaheuristic outer level is that the overall objective can become a nonlinear cost function as long as the nonlinearity is caused by the decision variables of the metaheuristics level. This capability allows a much broader range of cost functions; for example, it would allow program planners to apply a nonlinear penalty to the MILP solution as a function of the launch schedule, which would not be possible in a MILP-only approach. Another advantage of the proposed formulation is that it could be structured to facilitate uncertainties in the decision vector due to its generality in the form of the cost functions, though this is left for future work.

The results are validated and demonstrated with realistic case studies based on NASA's Apollo, Commercial Lunar Payload Services (CLPS) programs, and Artemis programs. These programs were chosen as case studies because of their complexity in terms of the wide range of payloads and logistics service providers. With NASA's recent approach of contracting out payload delivery to logistics service providers, it is important to maintain a centralized perspective on the available logistics vehicles in order to ensure that payload delivery contracts are awarded according to an efficient plan. This is particularly true when many of those payloads are in support of NASA's crewed exploration program, for which NASA maintains operational responsibility.

The rest of the paper is organized in the following way. First, Section II describes the two-layer optimization algorithm in detail, with Section II.B focusing on the metaheuristic schedule optimizer and II.C focusing on the commodity flow MILP. Then, the method is tested on a number of case studies in Section III. The commodity flow

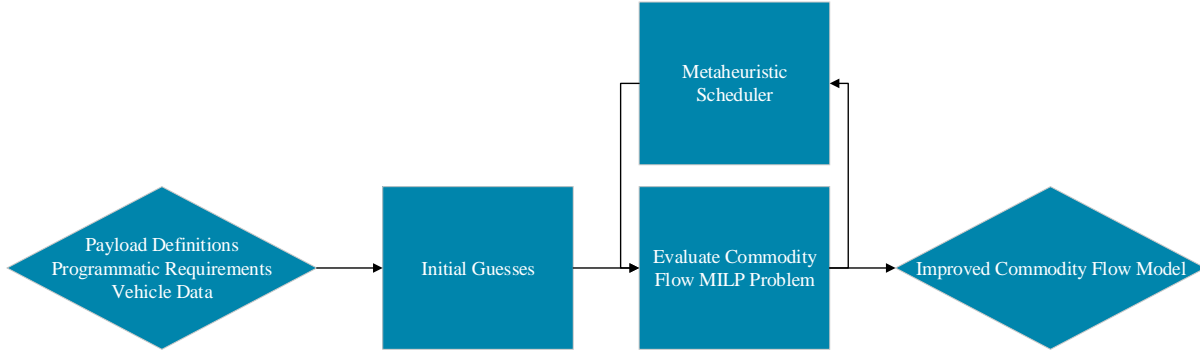


**Fig. 1 Overall structure of the generic campaign optimization problem [21].**

MILP is demonstrated in Section III.A using programmatic requirements based on an Apollo mission as input. In Section III.B, NASA’s CLPS program is studied as a demonstration of the scheduling algorithm. Finally in Sections III.C and III.D, the first phases (1, 2A, and 2B) of the Artemis program according to the GER are studied.

## II. Method

### A. Overview

The overarching method of the campaign planner is as follows:

- Vehicle design and campaign programmatic requirements are defined in input databases. The structure of the data is defined in Sections II.A.1 and II.A.2.
- A series of initial feasible guesses of the scheduling solutions are generated and used to initialize a genetic algorithm population. The decision variable contains the launch time of each payload in the campaign and this determines the network and the “demand matrix” of the logistics model.
- With each solution assessment, a MILP is constructed to solve the logistics optimization problem. If the model is feasible, it returns the total launch mass across the campaign as the objective to the genetic algorithm.

The evolutionary algorithm repeats this process in search of more optimal (minimized total launch mass) solutions. This workflow is illustrated in Figure 1.

#### 1. Vehicle Data

The vehicle data input database file contains a list of logistics vehicles that are available for the lunar exploration campaign. Table 1 lists the parameters associated with each vehicle. The "secondary" parameters are determined based on the values of  $I_{sp}$ , which is used as a proxy for propellant type.  $I_{sp} < 370$  was taken to be a storable propellant type,  $I_{sp} \geq 370$  s was taken to be cryogenic propellant. In this paper, our focus is on the chemical propulsion system, but the

**Table 1** Definitions of the input vehicle parameters.

Parameter	Description
$m_{\text{pay}}$	Payload capacity
$m_{\text{prop}}$	Propellant capacity
$m_{\text{dry}}$	Dry Mass
$I_{\text{sp}}$	Specific impulse
$t_F$	Launch frequency
$t_L$	Earliest allowed launch
$\mathcal{D}$	Domain: the set of arcs along which the vehicle is allowed to travel.
Secondary Parameter	Description
$\phi$	Propellant oxidizer mass ratio
$\beta$	Boil-off rate

**Table 2** Example vehicle data input.

Name	$m_{\text{pay}}$ , kg	$m_{\text{prop}}$ , kg	$m_{\text{dry}}$ , kg	$I_{\text{sp}}$ , s	$t_F$	$t_L$	$\mathcal{D}$
Vehicle 1	90	720	470	340	12	1	[0,0], [0,1], [1,2], [2,2], [2,3], [3,3]
Vehicle 2	1400	3320	1950	340	12	24	[0,0], [0,1], [1,2], [2,2]

work can be extended to other propulsion systems such as electric propulsion and nuclear thermal propulsion systems<sup>†</sup>. Throughout all case studies, the oxidizer boil-off rate was 0.016% loss per day for liquid oxygen and 0 for storable propellants. Fuel boil-off was neglected. Table 2 gives an example of vehicle data input format, in which Vehicle 1 is a small lander and Vehicle 2 is a larger service module.

In addition to the list of vehicles, a list of vehicle “stacks” is defined. A “stack” is an aggregation of individual space vehicles into a single unit, that can be assembled through rendezvous or disconnected. The vehicle stacking system implemented in the linear program was inspired by the ontologies developed by Trent, Edwards *et al.*, and Downs [23–25]. A vehicle stack is formatted as a list of its constituent vehicles and creates a new vehicle with the  $I_{\text{sp}}$  and domain of the leading element, which is taken to be the active element. For example, referring to the example vehicles in Table 2, if the stack [2,1] is allowed, then a new Vehicle 3 becomes the stack and has the domain and  $I_{\text{sp}}$  of Vehicle 2. Dry masses are summed together. The payload capability of the stack is the payload capability of the leading element minus the dry masses of the inactive elements.

## 2. Programmatic Requirements

The campaign program definition database file contains a list of payloads to be launched throughout the campaign. Table 3 lists the parameters associated with each payload. Payloads are indexed by  $l \in [0, N_p)$ , where  $N_p$  is the total number of campaign payloads. So, the first payload is  $l = 0$ , for example. The sets of pre- and co-payloads contain the indices of those payloads. The type indices are the same as those used in [9, 21]. Table 4 gives an example of the payload data input format.

<sup>†</sup>Note that for low-thrust electric propulsion, the trajectory design needs to be incorporated into the logistics design [22].

**Table 3 Definitions of the programmatic parameters.**

Parameter	Description
$p_l$	Payload type
$m_l$	Quantity/mass
$i_l$	Start node
$j_l$	Target node
$t_{L,l}$	Lower bound of launch window
$t_{U,l}$	Upper bound of launch window
$\mathcal{P}_l$	Set of soft precursors (payload $l$ must arrive <i>after or with</i> payloads in this set)
$\mathcal{Q}_l$	Set of strict precursors (payload $l$ must arrive <i>strictly after</i> payloads in this set)
$\mathcal{C}_l$	Set of co-payloads (payload $l$ must launch <i>with</i> payloads in this set)

**Table 4 Example payload data input.**

#	Name	Type Index	Quantity	Supply Node $i$	Demand Node $j$	$t_L$	$t_U$	Co-Payloads
0	Crew	1	2	0	3	0	12	
1	Science Payload	5	14	0	3	0	6	0

## B. Metaheuristics Layer

The “outer layer” of the optimization algorithm searches for optimal launch schedules. A genetic algorithm is used, where the decision vector  $\mathbf{x} \in \mathbf{Z}^{N_p}$  contains the launch time of each payload in the campaign. The integer time steps chosen by the metaheuristics are a month in length. This allows for simplified synergy with the periodic nature of the low-energy transfers.  $\mathbf{x}$  has the form  $\mathbf{x} = [t_0, t_1, \dots, t_{N_p}]$

The genetic algorithm searches for solutions to the problem stated in Equation (1), where  $\mathcal{F}$  is the output of the MILP, described in Section II.C, given the input schedule  $\mathbf{x}$  and set of programmatic requirements  $\mathcal{R}$ .  $\Lambda$  is a scaling factor on the MILP objective and is a function of the schedule, and  $\Gamma$  is a cost associated with the schedule. The use of a metaheuristic optimizer allows both  $\Lambda$  and  $\Gamma$  to be non-linear if necessary. For simplicity in the case studies, a one-to-one mapping between the MILP and metaheuristic objectives was used, i.e.,  $\Gamma = 0$  and  $\Lambda = 1$ . Section III.B.2 demonstrates a scheduling case with nonlinear  $\Gamma(\mathbf{x})$ .

$$\begin{aligned}
 \min_{t_l} \quad & \Lambda(\mathbf{x}(t_l), \mathcal{R})\mathcal{F}(\mathbf{x}(t_l), \mathcal{R}) + \Gamma(\mathbf{x}(t_l), \mathcal{R}) \\
 \text{s.t.} \quad & t_{L,l} \leq t_l \leq t_{U,l}
 \end{aligned} \tag{1}$$

The metaheuristics problem is subject to constraints imposed by the programmatic payload-sequencing requirements. Equations (2) - (4) list the constraints corresponding to the soft precursor, strict precursor, and co-payload requirements respectively. Soft precursors  $q$  must launch after, or with, the payload  $l$ , whilst strict pre-cursors must launch strictly after payload  $l$ . Co-payloads must launch at the same time as payload  $l$ .

$$t_q - t_l \leq 0 \quad \forall q \in \mathcal{P}_l \quad (2)$$

$$t_q - t_l < 0 \quad \forall q \in \mathcal{Q}_l \quad (3)$$

$$t_q - t_l = 0 \quad \forall q \in \mathcal{C}_l \quad (4)$$

The constraints are addressed indirectly by applying a “death penalty”, where a large positive scalar is assigned to the objective function value if the solution is infeasible, regardless of the extent of constraint violation [26]. Similarly, the death penalty is applied to any solution that, although feasible according to the metaheuristics constraints, is found to be infeasible by the MILP layer. The metaheuristic-layer optimization was carried out using the genetic algorithm of the pygmo [27] metaheuristic optimization python library.

### C. Logistics Mixed-Integer Linear Program (MILP) Layer

In space logistics, the transfer of vehicles, crew, payloads, and propellant are modeled as commodities flowing through a network. A mixed-integer linear program, an extension of the models described in [9, 21], is used to find the flow that results in a minimized launch mass, subject to certain constraints. Table 5 lists the constants, indices, and variables used in the linear program. Table 6 lists the locations represented in the model, and Table 7 lists the types of commodities and their costs. The cost of each commodity is its mass per unit.

The network describes the Earth, Moon, and various orbits as “nodes”, and the transfers between them as “arcs”. Each arc has a cost ( $\Delta V$ ) and a time-of-flight TOF associated with it. In a static network, only the nodes and the arcs representing their spatial separation are considered. The static network including the arc costs is shown in Figure 2. The arcs from the Earth node have zero  $\Delta V$  because it is assumed that a separate vehicle (the launcher) from the logistics vehicle would make these transfers. Launch vehicles are not tracked in this model, so the  $\Delta V$  from node 1 to node 2 is smaller than the reverse because it is assumed that the launch vehicle performs the lunar transfer injection, with the lander performing only the lunar orbit injection in that arc. The transfer from nodes 2 to 0 has a smaller  $\Delta V$  than the sum of 2 to 1 and 2 to 0 because the latter implies that the spacecraft actually inserts itself into LEO at node 1, whereas the former represents a direct atmospheric entry from the lunar return trajectory.

A network becomes “time-expanded” by repeating the static network across many discrete time steps, with “holdover” arcs connecting a location to its future counterpart. This is illustrated in Figure 3. The time expansion repeats with every second time step. That is to say,  $\tau_{i,j,0} = \tau_{i,j,2}$ . On these even time steps, only outbound flow is allowed. On odd time steps, return flow is allowed. A holdover arc on node 3 (lunar surface) from an even step to an odd step represents a

**Table 5** Definitions of the parameters, indices, and variables used in the linear program.

Parameters	Description
$N$	Total number of vehicles designs
$I$	Total number of network nodes
$P_I$	Number of integer commodity types
$P_F$	Number of float commodity types
$P = P_I + P_F$	Total number of commodity types
$T_{LP}$	Total number of time steps in the linear program
$C_{n,j,p,t}$	cost of launching commodity type $p$ , carried by vehicle $n$ , to node $j$ at time $t$ .
$d_{n,i,p,t}$	Demand matrix defining the supply (positive value) or demand (negative value) of commodity type $p$ , at node $i$ at time $t$ .
$Z_{n,i,j}$	Propellant mass fraction associated with vehicle $n$ travelling from node $i$ to node $j$ .
$c$	Crew consumables consumption rate
$\rho$	ISRU propellant production rate
$\mu$	ISRU maintenance supply requirement
$\tau_{i,j,t}$	Real time of flight between node $i$ and node $j$ at discrete time index $t$
$\mathcal{E}_{i,j}$	Boolean variable defining whether the arc from node $i$ to node $j$ exists.
Index	Description
$n \in [0, N)$	Vehicle
$i \in [0, I)$	Start node
$j \in [0, I)$	Final node
$p \in [0, P)$	Payload type
$io \in \{0, 1\}$	In-to- or out-of-arc
$t \in [0, T_{LP})$	Time
Variables	Description
$x_{n,i,j,p,io,t}$	Quantity of commodity type $p$ , carried by vehicle $n$ , from node $i$ to node $j$ at time $t$ .

**Table 6** Network nodes and arcs.

Node Index	Name	Arcs to
0	Earth Surface	0, 1
1	Low Earth Orbit (LEO)	0, 2
2	Low Lunar Orbit (LLO)	0, 1, 2, 3
3	Lunar Surface	2, 3

**Table 7 Payload types and their costs per unit used in the logistics formulation. Payloads 0 and 1 are integer quantities, and payloads 2 - 7 are continuous quantities.**

Index	Payload Type	Cost, kg per unit
0	Vehicle	$m_{\text{dry}}$
1	Crew	$m_{\text{crew}}$
2	ISRU Plant	1
3	Maintenance Supplies	1
4	Crew Consumables	1
5	Miscellaneous Non-Consumable Payload	1
6	Oxidiser	1
7	Fuel	1

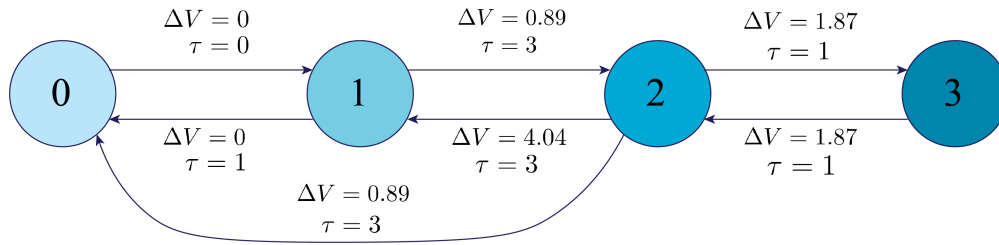


**Fig. 2 Diagram of the network model.  $\Delta V$  measured in  $\text{km s}^{-1}$ , values from [28]. Lunar ascent neglects gravity losses. Time of flight measured in days. Adapted from [21].**

short mission to the lunar surface, reminiscent of Apollo. The corresponding time of flight is 3 days. Meanwhile, the holdover arc in node 2 (lunar orbit) must equal the total of the time of flights for descent, surface stay, and ascent to maintain consistency, so its time of flight is 5 days. It is assumed that a long-duration mission would last some integer number of months, so the odd-to-even holdover arcs have time of flight such that 30 days have passed in total when returning to an even step. For example, a crew visiting the lunar surface takes 4 days to reach their destination. Then, a stay until the next macro-period adds 30 days. But, according to Fig. 3, the crew must stay another semi-period (+3 days), in order to use the return-direction arcs. Then, 4 days to return to the Earth make a total of a 41-day mission. Meanwhile, a crew that stays in LLO travels 3 days to reach LLO, then stays 30 days, after which 5 days takes them to the next semi-period, followed by 3 days to return, for a consistent 41-day mission. Longer duration stays would simply add multiples of the 30-day macro-period length.

Node 0 (Earth surface) has a holdover arc, but no associated time of flight, because time of flight is only used in consumable loss calculations and this is not considered to be relevant pre-launch.

The logistics MILP layer could be solved to optimize a variety of objectives, such as launch mass, launch cost, or fewest separate launches. For simplicity in the presented case studies, the logistics were optimized for minimized total mass to LEO, as this uses the simplest cost function. This is shown in Equation (5). For generality, the cost coefficient  $C$  is fully indexed for all nodes and all time, but with the stated objective, all coefficients are 0 unless  $j = 1$ , and with no

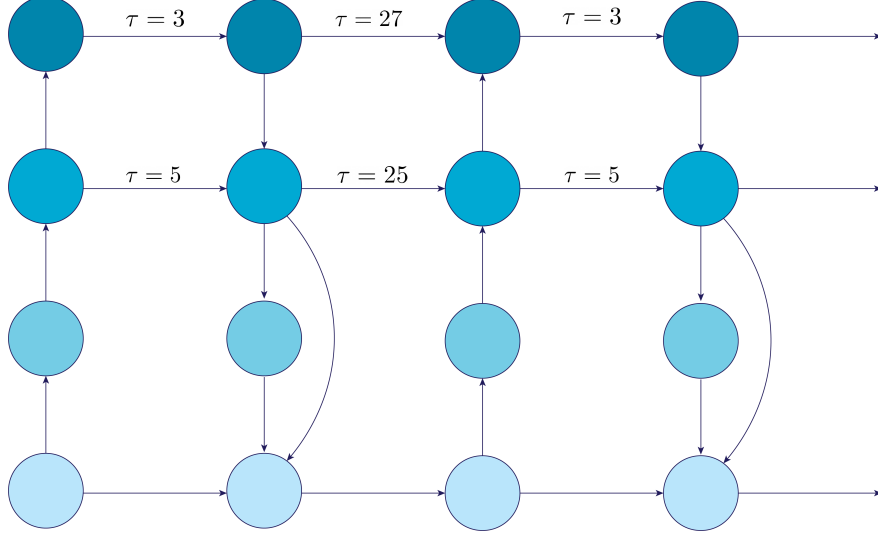


**Fig. 3** Diagram of the time-expanded network demonstrating the direction of commodity flow on each time step, including "time of flight"  $\tau$  of the holdover arcs. Time of flight measured in days.

variation with time.

$$\min_x f(x) = \sum_t \sum_n \sum_p \sum_j C_{n,j,p,t} x_{n,0,1,p,0,t} \quad (5)$$

In the following definitions, the model constraints have been arranged into 5 categories, within each of which the constraints have a shared purpose. Firstly, programmatic requirements are imposed on the commodity flow using a demand matrix  $d_{n,i,p,t}$ . This defines the supply or demand of commodities at specific nodes to be delivered at a specific time. Equations (6) and (7) state that the difference between the total amount of commodity flowing *into* a node from all others and the amount of the same commodity *leaving* the node to all others, is limited by the supply (positive value  $d$ ) or demand (negative value  $d$ ). Note that vehicles satisfy the demand/supply of their specific type, or vehicle stacks in which they appear,  $S'_n$ , whilst for all other payloads, only the sum of the payloads delivered by all logistics vehicles is considered. This allows commodities to transfer between vehicles but maintains proper supply rules for the vehicles themselves.

$$c_{1a}(x) : \sum_{n' \in S'_n} \sum_j (x_{n',i,j,p,0,t} - x_{n',j,i,p,1,t}) \leq d_{n,i,p,t} \quad \forall n, i, t, p = 0 \quad (6)$$

$$c_{1b}(x) : \sum_n \sum_j (x_{n,i,j,p,0,t} - x_{n,j,i,p,1,t}) \leq \sum_n d_{n,i,p,t} \quad \forall i, t, p > 0 \quad (7)$$

The second set of constraints enforce vehicle payload capacities. Crew, which are treated as integer payloads, have a mass (cost coefficient) of  $m_{\text{crew}}$  kg per crew member, whose value is assumed to be 100 kg in this paper. Spacecraft

have a cost coefficient equal to their dry mass. Payloads represented by continuous variables have a cost coefficient of 1. Note that the mass of the ISRU plants (index  $p = 2$ ) is excluded from the capacity for holdover arcs and the lunar surface as, in ISRU-based scenarios, they are intended to remain in place on the lunar surface independent of the movement of logistics vehicles.

$$c_2(x) : \begin{cases} m_{\text{crew}}x_{n,i,j,1,0,t} + \sum_{p=2}^5 x_{n,i,j,p,0,t} \leq m_{\text{pay},n}x_{n,i,j,0,0,t}, & \forall n, t, (i, j) : i \neq j \text{ or } i \neq 3 \\ m_{\text{crew}}x_{n,i,j,1,0,t} + \sum_{p=3}^5 x_{n,i,j,p,0,t} \leq m_{\text{pay},n}x_{n,i,j,0,0,t}, & \forall n, t, (i, j) : i = j = 3 \end{cases} \quad (8)$$

The third set of constraints, shown in Equations (9) and (10), impose the propellant capacity constraints.

$$c_{3a}(x) : x_{n,i,j,6,0,t} \leq x_{n,i,j,0,0,t} \phi_n m_{\text{prop},n} \quad \forall n, t, i, j \quad (9)$$

$$c_{3b}(x) : x_{n,i,j,7,0,t} \leq x_{n,i,j,0,0,t} (1 - \phi_n) m_{\text{prop},n} \quad \forall n, t, i, j \quad (10)$$

The fourth set of constraints ensure that changes in commodity quantities follow proper dynamics or conservation rules. Firstly, Equation (11) shows how crew consumables are consumed at a constant rate. In all case studies, a consumable rate of 8.655 kg per crew member per day was used, in consistency with [9].

$$c_{4a}(x) : x_{n,i,j,4,1,t} - x_{n,i,j,4,0,t} + c \tau_{i,j,t} x_{n,i,j,0,1,t} = 0 \quad \forall n, t, i, j \quad (11)$$

Equation (12) governs the maintenance supplies associated with ISRU infrastructure. The amount of maintenance supplies per day required is proportional to the mass of ISRU infrastructure present on the lunar surface.

$$c_{4b}(x) : \sum_n (x_{n,3,3,3,1,t} - x_{n,3,3,3,0,t} + \mu \tau_{3,3,t} x_{n,3,3,2,1,t}) = 0 \quad \forall t \quad (12)$$

Equations (13) and (14) describe oxidizer and fuel consumption when traveling over arcs. Holdover arcs (except the lunar surface) suffer from oxygen boil-off, which is modeled as a fractional loss-per-day  $\beta$ . Holdover arcs on the lunar surface ( $i = 3$ ) allow for refueling from ISRU-produced propellant, produced at a constant rate  $\rho$ . Transfer arcs are sufficiently short that boil-off was neglected.

$$c_{4c}(x) : \begin{cases} x_{n,i,j,6,1,t} - (1 - \beta_n)^{\tau_{i,j,t}} x_{n,i,j,6,0,t} = 0 & \forall n, t, (i, j) : i = j \neq 3 \\ x_{n,i,j,6,1,t} - x_{n,i,j,6,0,t} - \rho \tau_{i,j,t} \sum_n x_{n,i,j,2,1,t} = 0 & \forall n, t, (i, j) : i = j = 3 \\ x_{n,i,j,6,1,t} - x_{n,i,j,6,0,t}^+ \\ \phi_n Z_{n,i,j} \left( m_{\text{dry},n} x_{n,i,j,0,0,t} + m_{\text{crew}} x_{n,i,j,1,0,t} + \sum_{p=2}^7 x_{n,i,j,p,1,t} \right) = 0 & \forall n, t, (i, j) : i \neq j \end{cases} \quad (13)$$

$$c_{4d}(x) : \begin{cases} x_{n,i,j,7,1,t} - x_{n,i,j,7,0,t}^+ \\ (1 - \phi_n) Z_{n,i,j} \left( m_{\text{dry},n} x_{n,i,j,0,0,t} + m_{\text{crew}} x_{n,i,j,1,0,t} + \sum_{p=2}^7 x_{n,i,j,p,1,t} \right) = 0 & \forall n, t, i, j \end{cases} \quad (14)$$

Equation (15) states that other commodities are simply conserved across arcs.

$$c_{4d}(x) : x_{n,i,j,p,1,t} - x_{n,i,j,p,0,t} = 0 \quad \forall n, t, i, j, p \in \{0, 1, 3, 4, 5\} \quad (15)$$

The final set of constraints ensure, shown in Equation (16) that commodities only flow along arcs that exist at the current time step, and that vehicles remain within their domains.

$$c_5(x) : x_{n,i,j,p,io,t} = \begin{cases} 0 & \forall p, io, t, (n, i, j) \notin \mathcal{D}_n \\ 0 & \forall n, p, io, t, (i, j) : \mathcal{E}_{i,j} = 0 \\ 0 & \forall n, p, io, (i, j) : i > j \text{ and } t \text{ even} \\ 0 & \forall n, p, io, (i, j) : i < j \text{ and } t \text{ odd} \\ \text{unconstrained otherwise} \end{cases} \quad (16)$$

To summarize, the MILP problem solved is shown in Equation (17).

$$\begin{aligned} \min_x \quad & \text{Eqn. (5)} \\ \text{s.t.} \quad & \text{Eqns (6) ~ (15)} \end{aligned} \quad (17)$$

The MILP-layer commodity flow optimization was carried out using the Gurobi optimization software [29].

#### D. Model Construction

Two aspects of the commodity flow model change between iterations: the timeline, and the demand matrix. Both of these are determined by the decision vector chosen by the metaheuristic layer. Firstly, the metaheuristic chooses time stamps for each payload relative to the campaign timeline. The number of steps in the MILP timeline  $T_{LP}$  is equal to two times (outbound and return) the number of unique values in the metaheuristic decision vector  $\mathbf{x}(t_l)$ . So, for example, in a 12-month campaign, if payload 0 launches in the third month, then  $t_0 = 2$  (indexing starts at 0). The MILP, however, only cares about time steps where events happen. So if another payload 1 launches in month 7,  $t_1 = 6$ , then the MILP does not consider what happens on months 0, 1, 3, 4, or 5. So, the 12-month campaign timeline is mapped onto a reduced timeline, which in this case only has 4 time steps (the 2 steps where launches occur, and the half-steps allowing for return flows). Of course, the “real” (non-reduced) time that has passed must be tracked between the reduced steps, so that consumable calculations are made properly. So for every time step that was cut from the campaign timeline when producing the reduced timeline, 30 days are added to the “time of flight” of the corresponding holdover arcs.

The demand matrix is generated by creating positive demands (supplies) at the source nodes specified in the programmatic input data, and negative demands at the targets nodes, of the quantity and type of payload specified, at the time indicated in the metaheuristic decision vector. Vehicles are also supplied according to the vehicle data file. One unit of a vehicle is supplied at Earth on its first available timestep, and subsequent units are supplied with every multiple of that vehicles launch frequency. If a timestep in the reduced timeline corresponds to multiple launch frequency periods of that vehicle, then the model construction algorithm calculates how many units should be added at the next step. The MILP commodity flow model was constructed using the Pyomo python library [30, 31].

The overall flow of information between the different layers of the algorithm is shown in Figure 4.

#### E. Initial Feasible Guess Generation

The feasible space of the problem solved by the metaheuristic layer is very sparse, so it was necessary to create an algorithm that can generate pseudo-random (although naïve) initial feasible guesses, otherwise the feasible space is difficult to find. The guess generation method is summarised in Algorithm 1.

The objective of the algorithm is to find a launch time stamp for each payload in the programmatic requirements. It starts by checking the co-payload requirements, which if present would enforce a particular time stamp. If no co-payloads are found, then it checks for precursors. The allowed launch window is then updated with the new lower bound defined by the launch time of the most-constraining precursor. Then a random time stamp is chosen from the updated launch window. Finally, the algorithm checks that a suitable vehicle is available at this time stamp. If not, the launch window lower bound is set to the previous guess, and a new random-but-later time stamp is selected.

---

**Algorithm 1:** Initial feasible guess generator pseudo-code.

---

```
1 Input: Program and vehicles definitions.
2  $\mathbf{x} = \mathbf{0}$  // Initialize  $\mathbf{x}$  with 0's.
3  $\mathbf{v} = \text{rand}(0, N_v)$  // Initialize a list of vehicles assigned to each payload with random choices.
4 for  $i \in [0, N_P]$  do
5   if  $C_i \neq \emptyset$  then
6      $\mathbf{x}[i] = \mathbf{x}[j]$ ,  $j \in C_i$ 
7   else
8      $t_{L,i} = \max(t_{L,i}, \mathbf{x}[j] \forall j \in \mathcal{P}_i, \mathbf{x}[j] + 1 \forall j \in Q_i)$  // Update lower bound  $t_{L,i}$  of  $\mathbf{x}[i]$  to whichever is most
9     // constraining between its programmatic lower bound, or launch times of any necessary pre-cursors.
10    if  $t_{L,i} = t_{U,i}$  then
11       $\mathbf{x}[i] = t_{L,i} = t_{U,i}$  // Only one feasible choice of launch time.
12    else
13       $\mathbf{x}[i] = \text{rand}(t_{L,i}, t_{U,i})$  // If multiple choices are feasible, pick a random one.
14      // Next, it is necessary to check that there are usable vehicles available at this time stamp.
15      while Valid Vehicle Check is False do
16        // Maintain a list of vehicles which are valid for this payload. Initialize with full list
17        // of vehicles:
18        Valid Vehicle List =  $[0, N]$ 
19        if Payload origin node is Earth then
20          for  $n \in [0, N]$  do
21            if  $t_{L,n} > \mathbf{x}[i]$  then // Check that vehicle  $n$  is available at launch time  $\mathbf{x}[i]$ .
22              Remove vehicle  $n$  from the Valid Vehicle List.
23          if Valid Vehicle List  $\neq \emptyset$  then // If any valid vehicles remain, continue.
24            for  $n \in \text{Valid Vehicle List}$  do
25              Payload Mass =  $m_i C_i$  // Check that the payload capacity of each vehicle is not
26              // broken by adding this payload.
27              for  $j \in [0, i]$  do // Find other payloads launching at the same time, on vehicle  $n$ .
28                if  $\mathbf{x}[i] = \mathbf{x}[j]$  and  $\mathbf{v}[j] = n$  then
29                  Payload Mass +=  $m_j C_j$ 
30              if Payload Mass >  $m_{\text{pay},n}$  then // If the payload capacity of vehicle  $n$  is broken.
31                Remove vehicle  $n$  from the Valid Vehicle List.
32              if  $\mathbf{v}[j] = n$  and  $0 < |\mathbf{x}[j] - \mathbf{x}[i]| < t_{F,n}$  then // Check that the same vehicle is not used
33                // within a launch frequency period  $t_{F,n}$ 
34                Remove vehicle  $n$  from the Valid Vehicle List.
35          else
36            for  $n \in [0, N]$  do
37              if  $[3, 2] \notin \mathcal{D}_n$  or  $[2, 0] \notin \mathcal{D}_n$  then // If the payload is not sourced at Earth, it must be
38              // assigned to a return vehicle.
39                Remove vehicle  $n$  from the Valid Vehicle List.
40          if Valid Vehicle List  $\neq \emptyset$  then
41             $\mathbf{v}[i] = \text{rand}(\text{Valid Vehicle List})$ 
42            Valid Vehicle Check = True // Successfully found a valid vehicle for payload  $i$ .
43          else
44             $t_{L,i} = \text{rand}(t_{L,i}, t_{U,i})$  // If there are no valid vehicles, try a later time step.
45            if  $t_{L,i} \neq t_{U,i}$  then
46               $\mathbf{x}[i] = \text{rand}(t_{L,i}, t_{U,i})$ 
47            else
48               $\mathbf{x}[i] = t_{L,i}$ 
49
50 Output: Feasible design vector  $\mathbf{x}$ .
```

---

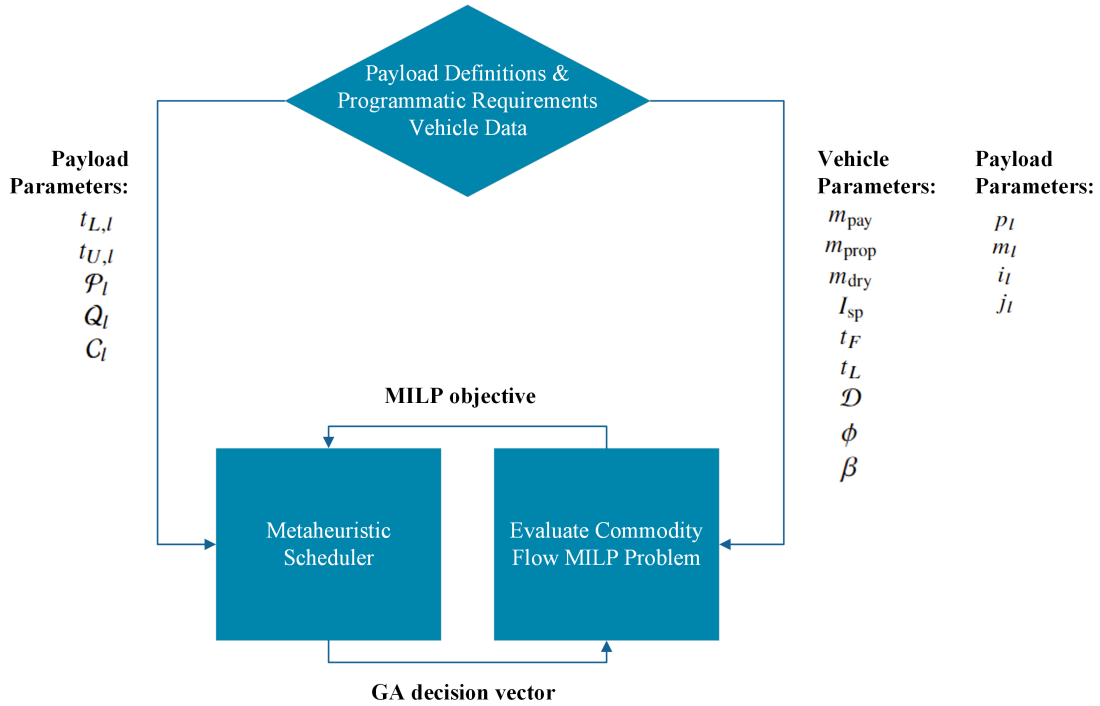


**Fig. 4 Flow of parameters and variables between the layers of the algorithm.**

### III. Results

This section will provide demonstration of both the commodity flow MILP and the metaheuristic scheduling algorithm. Then, the results of the Artemis program case studies will be presented and discussed.

#### A. Logistics MILP Demonstration Case: Apollo

Before moving on to the case studies, the commodity flow MILP is first demonstrated using a simple, single-mission Apollo study. In this simplified Apollo model, 3 astronauts are launched from Earth, with two headed for the lunar surface, and one remaining in lunar orbit. 10 kg of payload (representing a rock sample) are carried on the return leg. This programmatic data is summarized in Table 8, and the available vehicles are summarized in Table 9. The allowed vehicle stacks are [2, 0, 1] and [0, 1]. The linear program is provided with the input decision vector  $\mathbf{x}(t_l) = [0, 0, 0, 0, 0]$ , indicating that the mission is launched and returned within the same time step (month), corresponding to a 3 day lunar surface mission.

The output of the linear program is summarized in Figure 5. The returned objective value (total mass to LEO) is 37486 kg. This is not dissimilar to the values found by logistics MILP developed by Chen *et al* [9], with discrepancies being attributed to updates to the model and deviations in input. However, it is short of the 43572 kg mass at lunar orbit injection burn start of Apollo 11 quoted by ref. [32], due to the full inventory of payload and equipment not being included in this test.

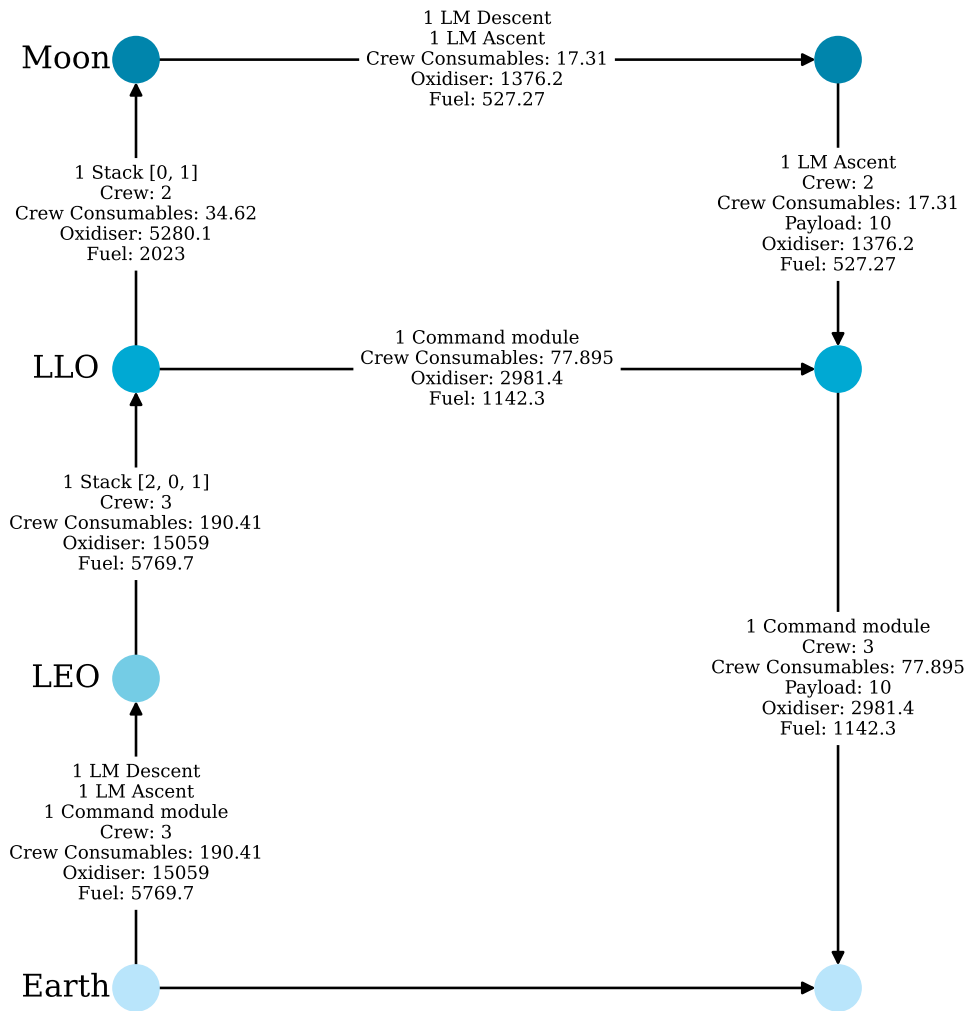


Fig. 5 Optimal commodity flow calculated by the MILP given the Apollo programmatic inputs.

**Table 8 Apollo payload data input.**

#	Name	Type Index	Quantity	$i$	$j$	$t_L$	$t_U$	Co-Payloads
0	Lunar Surface Crew	1	2	2	3	0	0	1
1	Lunar Orbit Crew	1	3	0	2	0	0	
2	Surface Crew Return	1	2	3	2	0	1	3
3	Orbit Crew Return	1	3	2	0	0	1	
4	Sample Return	5	10	3	0	0	1	2

**Table 9 Apollo vehicle data input. Lunar module (L.M.) data from [33], command module data from [32].**

#	Name	$m_{\text{pay}}$ , kg	$m_{\text{prop}}$ , kg	$m_{\text{dry}}$ , kg	$I_{\text{sp}}$ , s	$t_F$	$t_L$	$\mathcal{D}$
0	L.M. Descent Element	5300	8900	2217	311	1	0	[0,1], [2, 2], [2, 3], [3, 3]
1	L.M. Ascent Element	350	2670	2020	311	1	0	[0,1], [3, 3], [3, 2]
2	Command Module	22510	16870	11930	314.5	1	0	[0,1], [1,1], [1, 2], [2, 2], [2,0], [2,1], [1,0]

## B. Metaheuristic Scheduler Demonstration Case: Commercial Lunar Payloads Services (CLPS) Program

### 1. Demonstration with a Linear Cost Function

Next, the campaign scheduling aspect of the method is demonstrated by applying it to the NASA CLPS program. The CLPS program is a planned series of payloads to be delivered to the lunar surface by private companies. The payloads are a series of scientific missions that are in support of the following Artemis program. It should be noted, that the primary aim of program is to fund the development of a wide variety of commercial lunar landers for future robustness of lunar exploration campaigns, and is not optimized for the most efficient delivery of the payloads. This means, though, that it provides a relatively easy case study in which to attempt to optimize the schedule of the campaign.

In the following ConOps definitions, time  $t = 0$  corresponds to the month of December 2022. The list of CLPS payloads<sup>‡</sup> considered in this analysis is listed in Table 10, and the vehicles are listed in Table 11. Stacking is not allowed in this ConOps. Note that this is not an exhaustive list of CLPS vehicles, but those with sufficient publicly available data to build the model are included. Results will be compared to an assumed baseline scenario which is illustrated in Figure 6.

The schedule decision vector that corresponds to the baseline scenario of Figure 6 is:

$$\mathbf{x} = [11, 6, 11, 0, 6, 12, 13, 18, 25, 25, 36]$$

First, this vector is passed to the MILP which will solve the commodity flow optimization. The output commodity flow is shown in Figure 7, with an objective value of 19061 kg. Note that the vehicle assignments here do not match those assumed in the baseline scenario - this is because the vehicles themselves are treated as commodities, so

<sup>‡</sup>With the addition of Lunar Flashlight. Although not a CLPS payload, it is included as it launched as a co-payload of the inaugural ispace launch.

**Table 10 Payload data used in the CLPS analysis. Data quoted from sources where possible, and best approximations made otherwise. Time indices correspond to months with  $t = 0$  being December 2022. From [21]. Payload mass estimations were made according to publicly available information as of December 2022.**

#	Name	Type Index	Quantity	$i$	$j$	$t_L$	$t_U$	Co-Payloads $C$
0	First shared payloads [34]	5	14	0	3	0	12	
1	First shared payloads	5	14	0	3	0	12	
2	CLPS-1 [34, 35]	5	50	0	3	0	12	0
3	Lunar Flashlight	5	12	0	2	0	12	
4	CLPS-2 [34, 35]	5	50	0	3	0	12	1
5	CLPS-3 / PRIME-1 [35, 36]	5	36	0	3	7	12	
6	CLPS-4 [35]	5	300	0	3	13	13	
7	CLPS-5 [35]	5	50	0	3	13	24	
8	VIPER [35, 37]	5	430	0	3	12	25	
9	Mare Crisium mission [35, 38]	5	94	0	3	13	25	
10	Schrödinger mission [35, 39]	5	95	0	3	25	36	

**Table 11 Lunar lander data used in the CLPS analysis. Data quoted from sources where possible, and best approximations made otherwise. For example, assumptions about launch mass have been made based on the assumed launch vehicle in some cases. Time indices correspond to months with  $t = 0$  being December 2022. Adapted from [21].**

#	Name	$m_{\text{pay}}$ , kg	$m_{\text{prop}}$ , kg	$m_{\text{dry}}$ , kg	$I_{\text{sp}}$ , s	$t_F$	$t_L$	$\mathcal{D}$
0	Astrobotic "Peregrine" [40]	90	720	470	340	12	1	[0,0], [0,1], [1, 2], [2,3], [3,3]
1	Astrobotic "Griffin" [41, 42]	630	3320	1950	340	12	24	[0,0], [0,1], [1, 2], [2,3], [3,3]
2	B.O. "Blue Moon" [43, 44]	4500	6350	2150	420	12	24	[0,0], [0,1], [1, 2], [2,3], [3,3]
3	ispace S1 [45]	30	700	300	340	12	0	[0,0], [0,1], [1, 2], [2,3], [3,3]
4	Draper/ispace S2 [46]	500	3380	2120	340	12	13	[0,0], [0,1], [1, 2], [2,3], [3,3]
5	Firefly "Blue Ghost" [47]	155	3380	2470	340	12	13	[0,0], [0,1], [1, 2], [2,3], [3,3]
6	I.M. "Nova-C" [48]	100	1010	790	370	6	0	[0,0], [0,1], [1, 2], [2,3], [3,3]
7	L.M. "McCandless" [49]	350	3380	2270	340	12	48	[0,0], [0,1], [1, 2], [2,3], [3,3]
8	M.E. MX-1 "Scout" [50]	30	150	70	320	12	48	[0,0], [0,1], [1, 2], [2,3], [3,3]

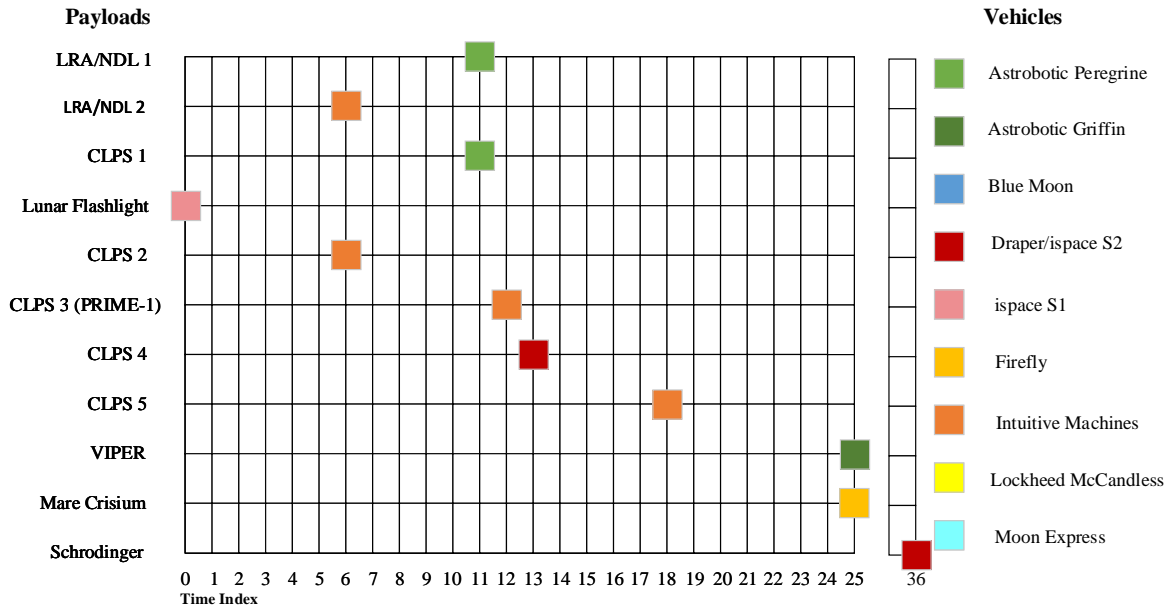


**Fig. 6 Assumed baseline schedule and vehicle assignments of the CLPS campaign. Adapted from [21], based on assumptions made from publicly available data as of December 2022. Updated with real-world delays as of May 2023.**

payload-to-vehicle assignment is optimized at the MILP level.



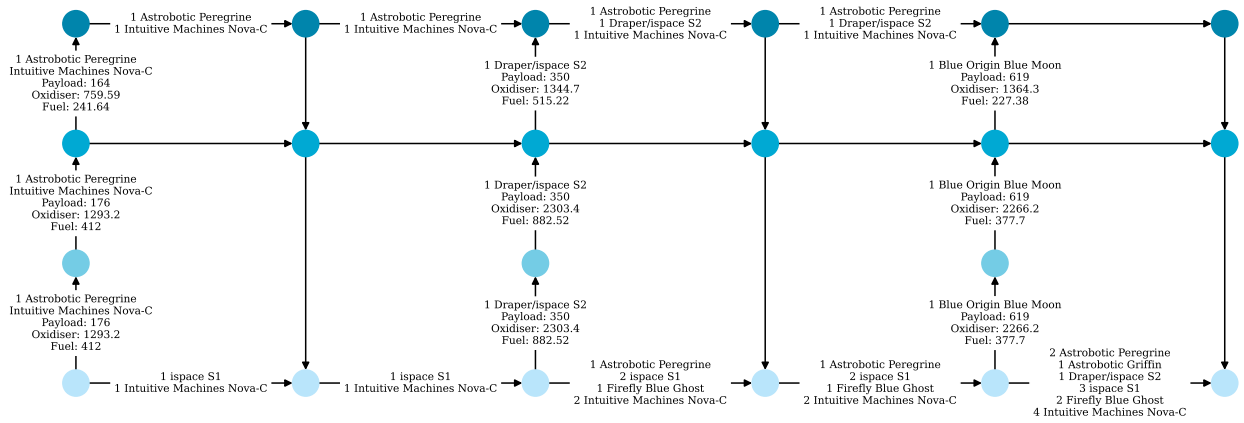


**Fig. 8 CLPS ConOps with both optimized schedule and optimized commodity flow.**

Next, the overall campaign is optimized using the metaheuristic schedule optimizer. This was done by generating 20 initial feasible guesses using Algorithm 1 and using them to initialize the genetic algorithm population. 5 such populations were initialized as pygmo “island” objects. Islands are a framework for parallelized function evaluation with metaheuristic optimization algorithms [51]. Then, the genetic algorithm evolved the “archipelago” of islands through 200 generations with a mutation probability of 0.05. With each generation, the best solutions can migrate between islands, providing a form of parallelized evolution. The best-found solution through this evolution returned an objective of 14207 kg, which was found after 29 generations / 580 MILP evaluations. The commodity flow for the optimized launch schedule is shown in Figure 8.

As stated in the introduction, commodity flow LPs can handle scheduling with constraints no more complex than upper and lower bounds. Therefore, the CLPS case study also serves as a demonstration case for the scheduling algorithm, as the scheduling requirements are simple enough that they can be handled directly by the logistics MILP algorithm if Payloads 0 and 1 from Table 10 are directly combined with payloads 2 and 4 such that the co-payloads requirements  $C$  were enforced. The new model was constructed by creating a new demand matrix in which the supply time is defined as the lower bound of the payload’s availability window  $t_L$  and the demand time is defined as the upper bound of the availability window  $t_U$ . When this new model is solved, an objective of 14207 kg is found, verifying that the scheduling algorithm found an optimal schedule.

The optimized schedule represents a mass saving of 4854 kg across the campaign. This saving is somewhat short of the equivalent of a dedicated Falcon 9 (or similar) launch. But, it would save on the cost of multiple ride-share missions of the smaller lunar logistics vehicles. This is evidenced by the fact that the total number of launches required was reduced from 7 down to 3.

## 2. Demonstration with a Nonlinear Cost Function

One of the advantages of using metaheuristic scheduler over existing MILP-based approaches is the possibility to incorporate a nonlinear cost function. To showcase this unique advantage, this subsection details a schedule optimization featuring a nonlinear cost function. As a simple example case, the same CLPS campaign was re-evaluated, this time including an exponential penalty function that penalizes against payloads launching at the same time, shown in Equation (18). Here, the penalty function of Equation 1 becomes  $\Gamma = \alpha \exp(\mathcal{N}(t_l))$ , where  $\mathcal{N}(t_l)$  is the number of non-unique entries listed in  $\mathbf{x}(t_l)$  (i.e., penalizing launching two or more payloads at the same time step), and  $k$  is a scaling coefficient. Besides the updated objective, the same constraints as previously described were maintained.

$$\min_{t_l} \mathcal{F}(\mathbf{x}(t_l), \mathcal{R}) + k \exp(\mathcal{N}(t_l)) \quad (18)$$

With this new objective, the optimization process of Section III.B was repeated. The new best found decision vector was:

$$\mathbf{x} = [7, 3, 7, 10, 3, 12, 13, 18, 25, 20, 35]$$

As expected, the algorithm returns a decision vector with minimal repeated co-manifested launches. The unpenalized commodity flow objective was 20764 kg. For the rest of the paper, the linear cost function is used as the nominal case.

### C. Case Study 1: Artemis Phases 1 and 2A

The first full case study expands the CLPS case to include the lunar surface missions of Artemis Phases 1 and 2A. Artemis Phase 1 is assumed to include the CLPS missions and the first crewed lunar landing (Artemis 3). Phase 2A then consists of the following surface missions up to Artemis 6. Artemis missions 3 - 5 are all 3 day missions (in terms of the timeline used in the metaheuristic scheduling algorithm, the return missions happens in the same time step as the outbound), whereas Artemis 6 is required to be at least a month long. Artemis 5 has the pressurized crew rover as a pre-requisite payload. The list of payloads in the campaign is appended with those listed in Table 12 and the list of available vehicles is appended with those in Table 13. The allowed vehicle stacks are [12, 10, 11], [10, 11], and [12, 11].

Again, an initial population of 20 random feasible guesses was generated using Algorithm 1, and used to populate 5 islands. The islands were evolved through 400 generations, again with cross-migrations. In this analysis, a smaller mutation probability of 0.01 was used. This is because the decision vector is larger, due to the larger list of payloads, so there are more opportunities for mutations to occur. The smaller probability was used to balance this so that the overall mutation rate did not increase.

The full details of the best found solution are shown in Figure 9 (from here onward, unused vehicles remaining at the Earth node will not be shown for simplicity), and Table 14 summarizes the key findings. The solution shows a quirk

**Table 12** Additional payload data used in the Artemis phase 1 and 2A analysis. Data quoted from sources where possible, and best approximations made otherwise. Time indices correspond to months with  $t = 0$  being December 2022. From [21]. Payload mass estimations were made according to publicly available information as of December 2022.

#	Name	Type Index	Quantity	$i$	$j$	$t_L$	$t_U$	$\mathcal{P}$	$Q$	$C$
11	LUPEX [52]	5	350	0	3	25	36			
12	LEAP Rover [53]	5	30	0	3	37	48			
13	Unpressurised Crew Rover	5	300	0	3	12	24			
14	Artemis 3 Launch	1	2	0	2	24	39			
15	Artemis 3 Landing	1	2	2	3	24	39			14
16	Artemis 3 Ascent	1	2	3	2	24	39			14
17	Artemis 3 Return	1	2	2	0	24	39			14
18	Artemis 4 Launch	1	2	0	2	40	55			
19	Artemis 4 Landing	1	2	2	3	40	55			18
20	Artemis 4 Ascent	1	2	3	2	40	55			18
21	Artemis 4 Return	1	2	2	0	40	55			18
22	ISRU demo	2	300	0	3	37	49			
23	Small Pressurised Rover	5	4000	0	3	56	71			
24	Artemis 5 Launch	1	2	0	2	56	71	23		
25	Artemis 5 Landing	1	2	2	3	56	71			24
26	Artemis 5 Ascent	1	2	3	2	56	71			24
27	Artemis 5 Return	1	2	2	0	56	71			24
28	Artemis 6 Launch	1	4	0	2	72	87			
29	Artemis 6 Landing	1	4	2	3	72	87			28
30	Artemis 6 Ascent	1	4	3	2	72	87	28		
31	Artemis 6 Return	1	4	2	0	72	87			30

**Table 13** Additional lunar lander data used in the Artemis phase 1 and 2A analysis. Data quoted from sources where possible, and best approximations made otherwise. The figures regarding the Orion spacecraft differ from the real-world equivalent because this model requires that Orion deliver its crew to LLO, rather than the real-world requirement of higher lunar orbits such as near-rectilinear halo orbits. Time indices correspond to months with  $t = 0$  being December 2022. Adapted from [21].

#	Name	$m_{\text{pay}}$ , kg	$m_{\text{prop}}$ , kg	$m_{\text{dry}}$ , kg	$I_{\text{sp}}$ , s	$t_F$	$t_L$	$\mathcal{D}$
9	ESA EL3 [54]	1800	5580	2520	340	24	84	[0,1], [1, 2], [2,3], [3,3]
10	ISECG lander [55]	9000	23660	9340	340	12	12	[0,0], [0,1], [2,2], [2,3], [3,3]
11	ISECG ascender	500	10000	1000	340	12	12	[0,0], [0,1], [3,3], [3,2]
12	Orion	11800	22000	16520	316	12	0	[0,0], [0,1], [1,1], [1,2], [2,2], [2,0], [2,1], [1,0]
13	JAXA/ISRO lander [52]	350	3510	2140	320	36	25	[0,1], [1, 2], [2,3], [3,3]

of the commodity flow model in that, in December 2027, the crew are launched on CLPS vehicle and rendezvous with a pre-launched Orion capsule in lunar orbit. The commodity flow solver chose this solution because it is agnostic to whether a vehicle is a crew-rated or not, and the Blue Origin lander has the highest  $I_{sp}$  of the available vehicles. Though this could easily be implemented in future models if necessary, it does of course indicate the value of high- $I_{sp}$  crewed vehicles.

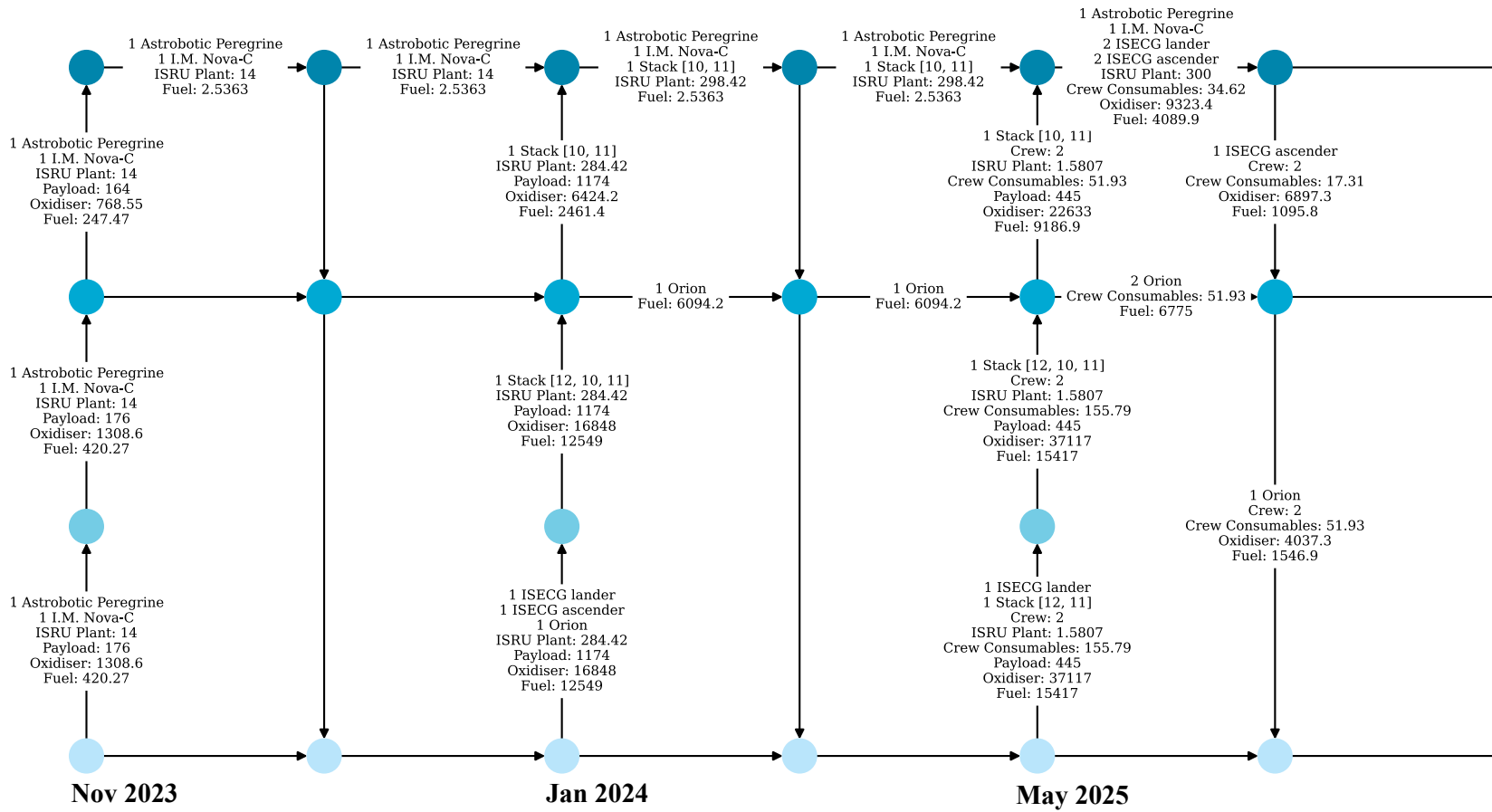
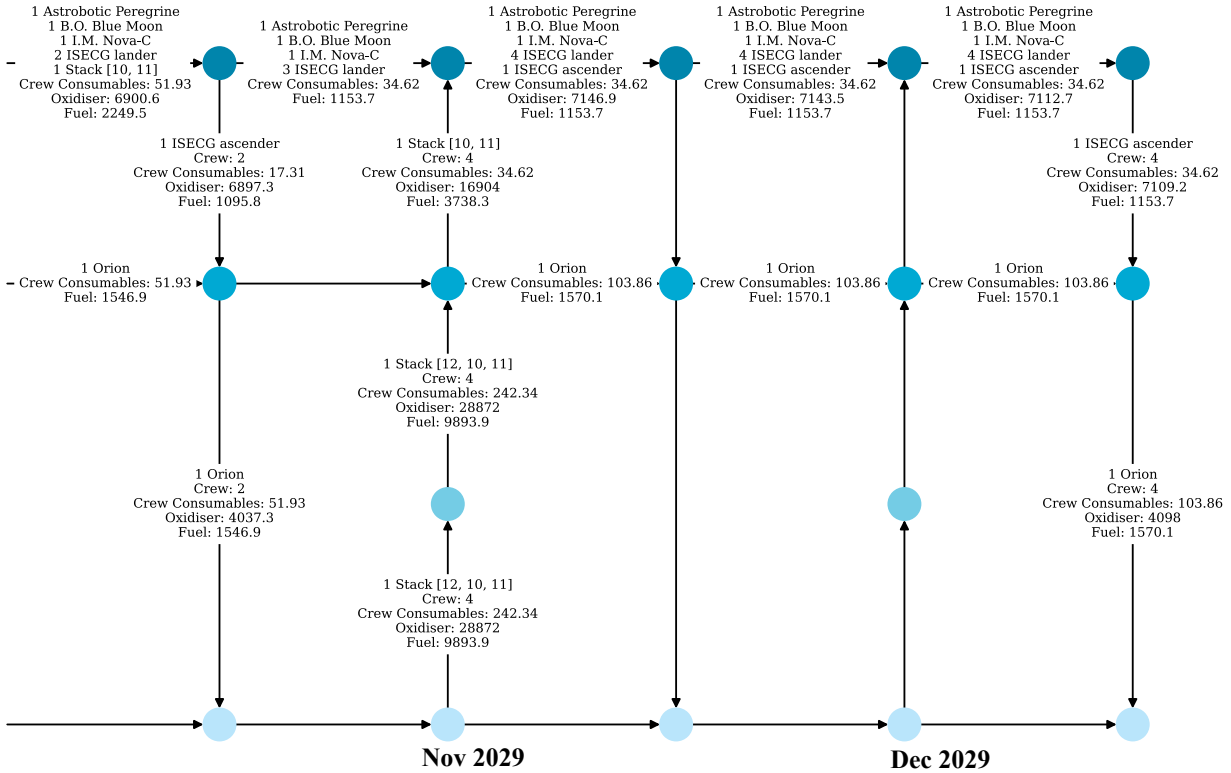


Fig. 9 (continued on next page).





**Fig. 9 Artemis phase 1 and 2A ConOps with optimized schedule and optimized commodity flow.**

Table 15 summarizes the number of times that vehicles were used in the optimized Artemis phase 1 and 2A ConOps. It can be seen that the optimal solution features only a small number of the available vehicles, with the optimal strategy typically being to include as many payloads in the larger capacity crewed launches as the programmatic requirements allow. It follows that the best-performing solutions are sensitive to the availability of those larger logistics vehicles. Any disruption to their availability frequency, or earliest availability, could render the best solutions infeasible. Although the unused vehicles do not contribute to the optimal results within the considered constraints, they would have usefulness in terms of robustness against certain aleatory uncertainties such as payload development delays.

**D. Case Study 2: Artemis Phase 2B**

A major advantage of the development of time-expanded commodity flow models for space logistics [7, 9] is the ability to model the impact that *in-situ* resource utilization (ISRU) infrastructure has on the overall logistics of a campaign. In summary, resources found on the lunar surface can be taken advantage of and used to produce materials that are useful to the exploration campaign, with the objective of reducing the overall mass of material required to be launched from Earth. In particular, this method studies the impact of producing propellant from water ice on the lunar surface.

This final case study looks to demonstrate how this can improve longer-term campaign planning and scheduling, in

**Table 14 Summary of the Artemis 3 - 6 mission schedules, including pre-launched and co-manifested payloads.**

Artemis Mission #	Launch Date	Pre-launched Supporting Payloads Name	Supporting Payloads Date	Co-manifested Supporting Payloads	
3	Outbound Return	May 2025	CLPS Payloads Unpressurized Rover ISRU Demo	Nov 2023, Jan 2024	CLPS Payloads
4	Outbound Return	Nov 2026			LEAP Rover
5	Outbound Return	Dec 2027			Small Pressurized Rover
6	Outbound Return	Nov 2029 Dec 2029			

**Table 15 Number of times each vehicle was used in the optimized Artemis phase 1 and 2A ConOps.**

Name	No. times used
Astrobotic Peregrine	1
I.M Nova-C	1
B.O. Blue Moon	1
ISECG lander	4
ISECG ascender	4
Orion	4

addition to testing a more complex set of programmatic requirements with a much larger solution space. To do this, the case study will consider the Artemis Phase 2B scenario, building towards the sustainable permanent lunar outpost of Artemis Phase 3, or the "Moon Village" concepts [56]. It features the delivery of large habitation and power generation elements, and pressurized rovers. Phase 2B includes crewed missions 7 through 14, each with large sample return masses. Finally, because the impact of ISRU on the campaign was to be studied, "Mk 2" versions of the ISECG vehicles were added to the scenario, each assumed to have the same dry masses and propellant capacities but with upgraded  $I_{sp}$  of 370s, indicating the upgrade to ISRU-compatible cryogenic propellant. The payload capabilities of the lander were expanded accordingly with the new  $I_{sp}$ .

In the following analysis, an ISRU infrastructure maintenance supply delivery rate of 10% of the total infrastructure mass per year is used. The rate of production of *in-situ* produced oxygen was calculated using the parametric sizing model developed by Schreiner *et al* [57]. Ref. [57] offers values for reactor mass and power requirements as a function of production rate. Based on this, a relatively conservative production rate value of 2000 kg oxygen per year per 500 kg of reactor mass is chosen, with a power requirement of 10 W per kg oxygen per year. The power requirement is then converted to a power system mass using data from the NASA Small Fission Power System study [58], which offers expected specific power (W per kg) for multi-kW capable, lunar surface fission reactors. A specific power of 6.5 W per kg is used here. With values for reactor mass, reactor power requirements, and power system mass, the total resource

production rate per ISRU infrastructure mass can be calculated. With the quoted values, the resulting ISRU oxygen production rate is  $\rho = 0.00153$  kg oxygen per day per kg of infrastructure.

The Artemis Phase 2B campaign is defined in this analysis by the list of payloads in Table 16. These payloads are adapted from [59].  $t = 0$  is undefined, assumed to be some date later than the December 2029 end date of the Artemis 1 and 2A analysis. The same list of vehicles from the previous case studies is used again, with the lower bound of availability removed, as this campaign is further in the future. The additional Mk 2 ISECG vehicles are listed in Table 17. Additional vehicle stacks are defined such that the Mk2 landers can stack together, as well as mixed stacks of Mk1 and Mk2 landers.

20 initial feasible guesses were generated using Algorithm 1. These guesses were used to initialize two metaheuristic algorithm populations. Only two population islands were used in this analysis because of the larger computing power requirements of the increased model size. A mutation probability of 0.01 was used.

After evolution through 40 generations, the objective value improved from 886750 kg to 819650 kg. The full commodity flow produced by this improved solution is shown in Figure 10, and the key findings are summarized in Table 18. The relative saving of 67100 kg is the equivalent of  $\approx 1.75$  crewed SLS Block 1B launches [60]. The evolution that the best-found objective takes over the course of the metaheuristic optimization, shown in Figure 11, gives some insight into the effectiveness of intermediate points between the manually-found solution and the best-found solution. Although, due to the stochasticity of genetic algorithms, these insights are not definite statements. The initial sharp improvement in the objective shows that the manually-found solution was a relatively poor one. Then, the algorithm moves through a series of small improvements, likely indicating that a number of closely related solutions exist in the design space.

To analyze the structure of the problem further, it is clear that families of solutions could exist. Given a particular solution, if the groupings of payloads that launch together and the launch sequence are both maintained, it is possible to adjust the time indices of individual launches within their bounds and maintain a feasible solution, as long as vehicle supply constraints are respected. In this case study, the flexibility and robustness of the solution are not analyzed further and are left for future work. However, the method presented here is useful for finding good baseline solutions to the launch sequencing and payload groupings, after which minor tweaks to the schedule could be made by the program architect.

**Table 16 Payload data used in the Artemis phase 2B analysis. Adapted from [59].**

#	Name	Type Index	Quantity	$i$	$j$	$t_L$	$t_U$	$\mathcal{P}$	$Q$	$C$
0	Power Plant element	5	1500	0	3	0	48			
1	Artemis 7 Crew	1	4	0	2	0	48	0		
2	Artemis 7 Crew Landing	1	4	2	3	0	48			1
3	Artemis 7 Crew Ascent	1	4	3	2	0	48		2	
4	Artemis 7 Crew Return	1	4	2	0	0	48			3
5	Sample return	5	200	3	0	0	48			
6	Habitat	5	4500	0	3	0	54			
7	Artemis 8 Crew	1	4	0	2	0	54	6	4	
8	Artemis 8 Crew Landing	1	4	2	3	0	54			7
9	Artemis 8 Crew Ascent	1	4	3	2	0	54		8	
10	Artemis 8 Crew Return	1	4	2	0	0	54			9
11	Sample return	5	200	3	0	0	54			
12	Artemis 9 Crew	1	4	0	2	12	60		10	
13	Artemis 9 Crew Landing	1	4	2	3	12	60			12
14	Artemis 9 Crew Ascent	1	4	3	2	12	60		13	
15	Artemis 9 Crew Return	1	4	2	0	12	60			14
16	Sample return	5	200	3	0	12	60			
17	Pressurised Rover	5	4500	0	3	0	66			
18	Pressurised Rover	5	4500	0	3	0	66			
19	Artemis 10 Crew	1	4	0	2	24	66	17, 18	15	
20	Artemis 10 Crew Landing	1	4	2	3	24	66			19
21	Artemis 10 Crew Ascent	1	4	3	2	24	66		20	
22	Artemis 10 Crew Return	1	4	2	0	24	66			21
23	Sample return	5	200	3	0	24	66			
24	Artemis 11 Crew	1	4	0	2	36	72		22	
25	Artemis 11 Crew Landing	1	4	2	3	36	72			24
26	Artemis 11 Crew Ascent	1	4	3	2	36	72		25	
27	Artemis 11 Crew Return	1	4	2	0	36	72			26
28	Sample return	5	200	3	0	36	72			
29	Artemis 12 Crew	1	4	0	2	48	84		27	
30	Artemis 12 Crew Landing	1	4	2	3	48	84			29
31	Artemis 12 Crew Ascent	1	4	3	2	48	84		30	
32	Artemis 12 Crew Return	1	4	2	0	48	84			31
33	Sample return	5	200	3	0	48	84			
34	Fission Power Plant	5	4500	0	3	48	84			
35	Habitat	5	4500	0	3	48	84			
36	Artemis 13 Crew	1	4	0	2	60	96	34, 35	32	
37	Artemis 13 Crew Landing	1	4	2	3	60	96			36
38	Artemis 13 Crew Ascent	1	4	3	2	60	96		37	
39	Artemis 13 Crew Return	1	4	2	0	60	96			38
40	Sample return	5	200	3	0	60	96			
41	Artemis 14 Crew	1	4	0	2	72	96		39	
42	Artemis 14 Crew Landing	1	4	2	3	72	96			41
43	Artemis 14 Crew Ascent	1	4	3	2	72	96		42	
43	Artemis 14 Crew Return	1	4	2	0	72	96			43
44	Sample return	5	200	3	0	72	96			

**Table 17 Mk 2 ISECG vehicles used in the Artemis 2B analysis.**

#	Name	$m_{\text{pay}}$ , kg	$m_{\text{prop}}$ , kg	$m_{\text{dry}}$ , kg	$I_{\text{sp}}$ , s	$t_F$	$t_L$	$\mathcal{D}$
14	MK2 ISECG lander	11390	23660	9340	370	12	0	[0, 0], [0,1], [2, 2], [2, 3], [3, 3]
15	MK2 ISECG ascender	500	10000	1000	370	12	0	[0, 0], [0, 1], [3, 3], [3, 2]

**Table 18 Summary of the Artemis 7 - 14 mission schedules, including pre-launched and co-manifested payloads.**

Artemis Mission #	Launch Time	Pre-launched Supporting Payloads Name	Supporting Payloads Time	Co-manifested Supporting Payloads	
7	Outbound	46	Power Plant	17	ISRU Plant
	Return	48	ISRU Plant		Maintenance Supplies
			Maintenance Supplies Pressurized Rover	39	
8	Outbound	52	Habitat	48	ISRU Plant
	Return	53			Habitat
9	Outbound	54	Pressurized Rover	53	
	Return	58			
10	Outbound	61			Fission Power Plant
	Return	64			
11	Outbound	68			
	Return	71			
12	Outbound	78			
	Return	83			
13	Outbound	88			
	Return	93			
14	Outbound	94			
	Return	95			

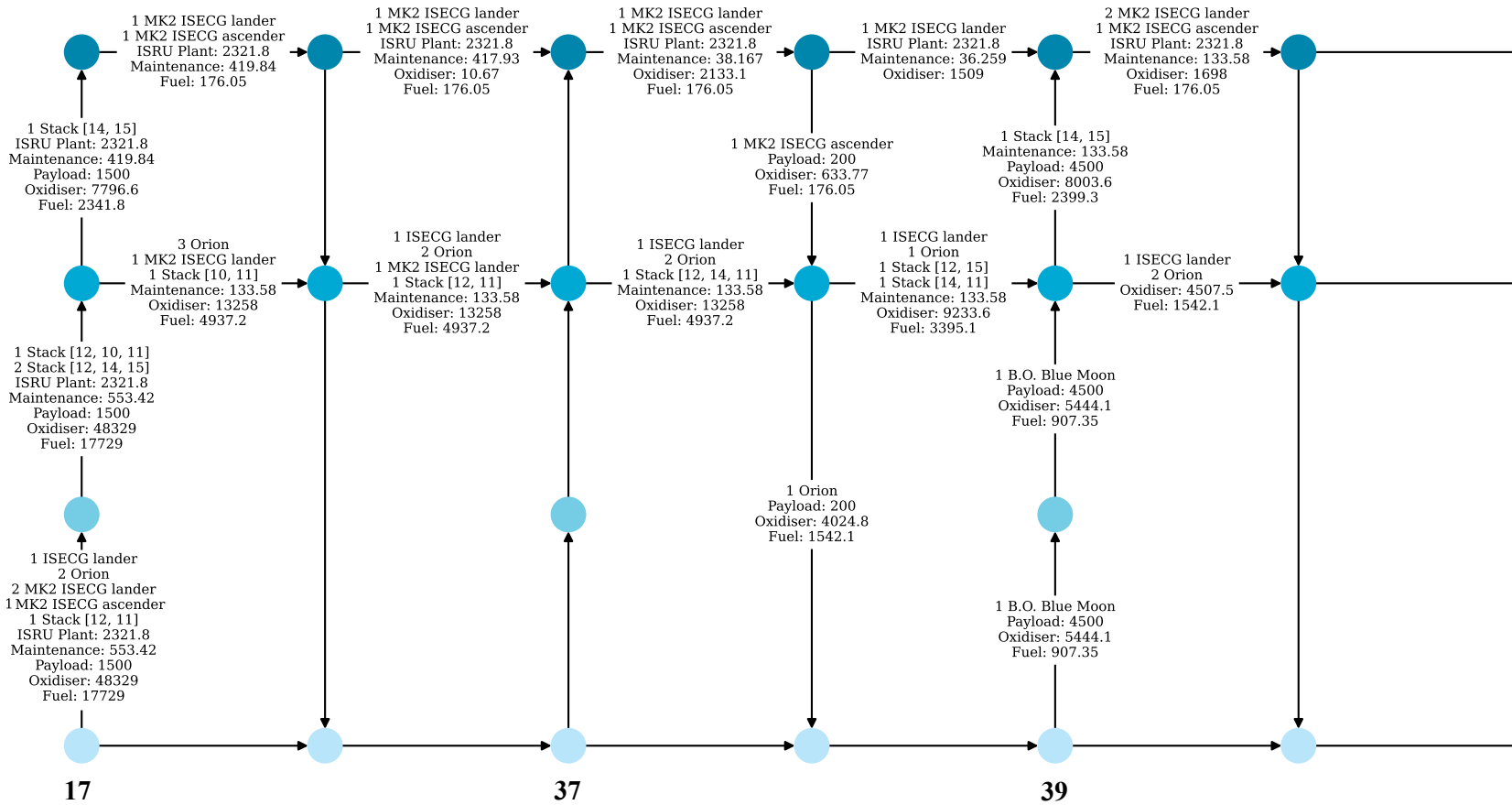


Fig. 10 (continued on next page).

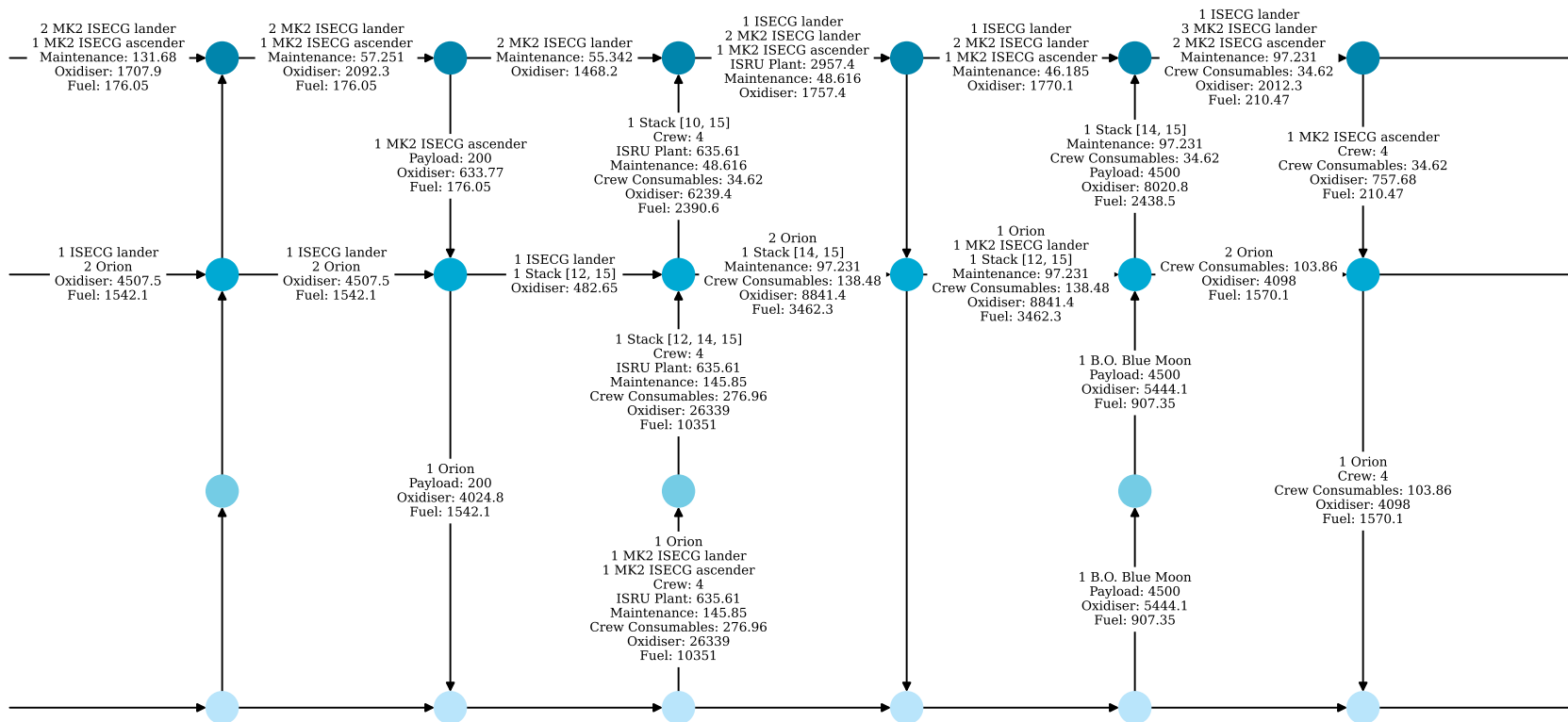


Fig. 10 (continued on next page).

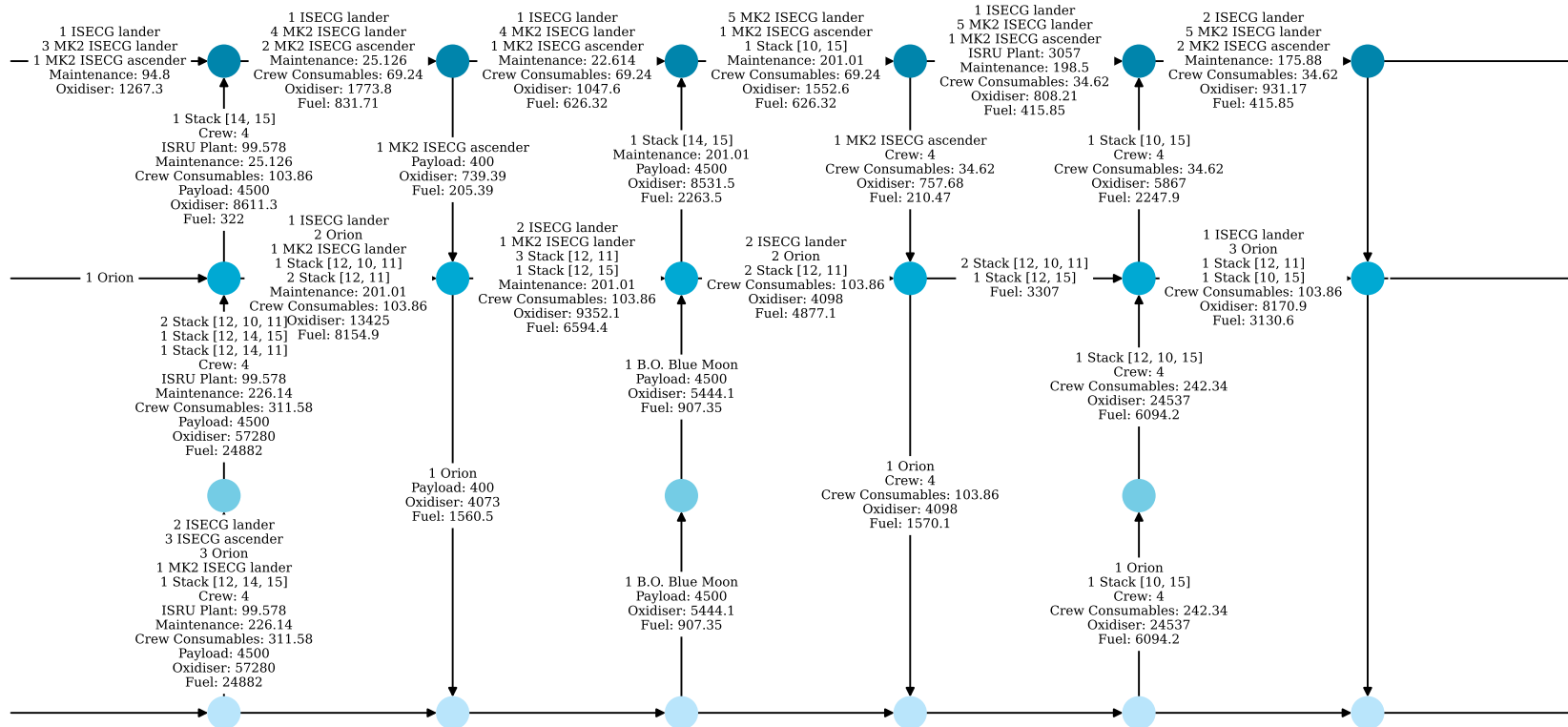


Fig. 10 (continued on next page).

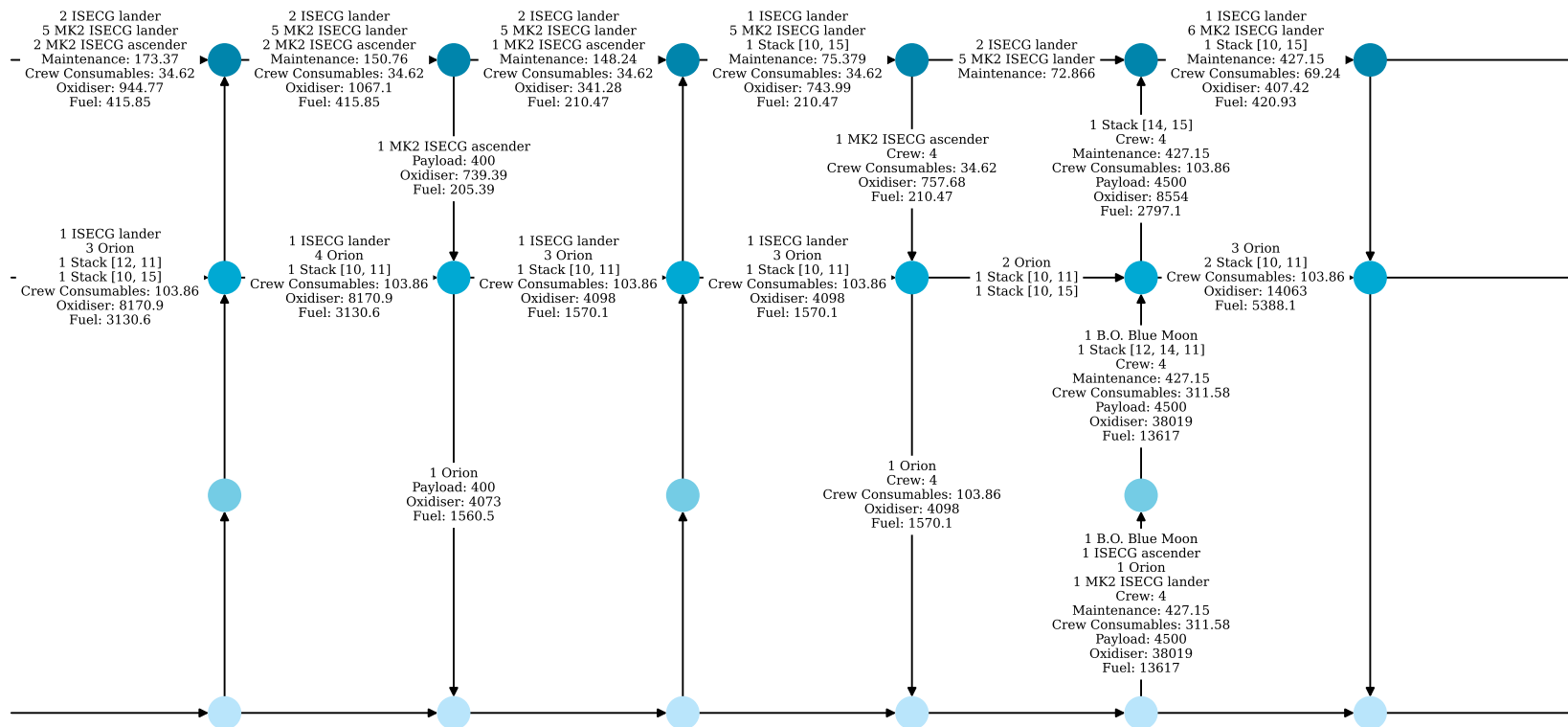


Fig. 10 (continued on next page).

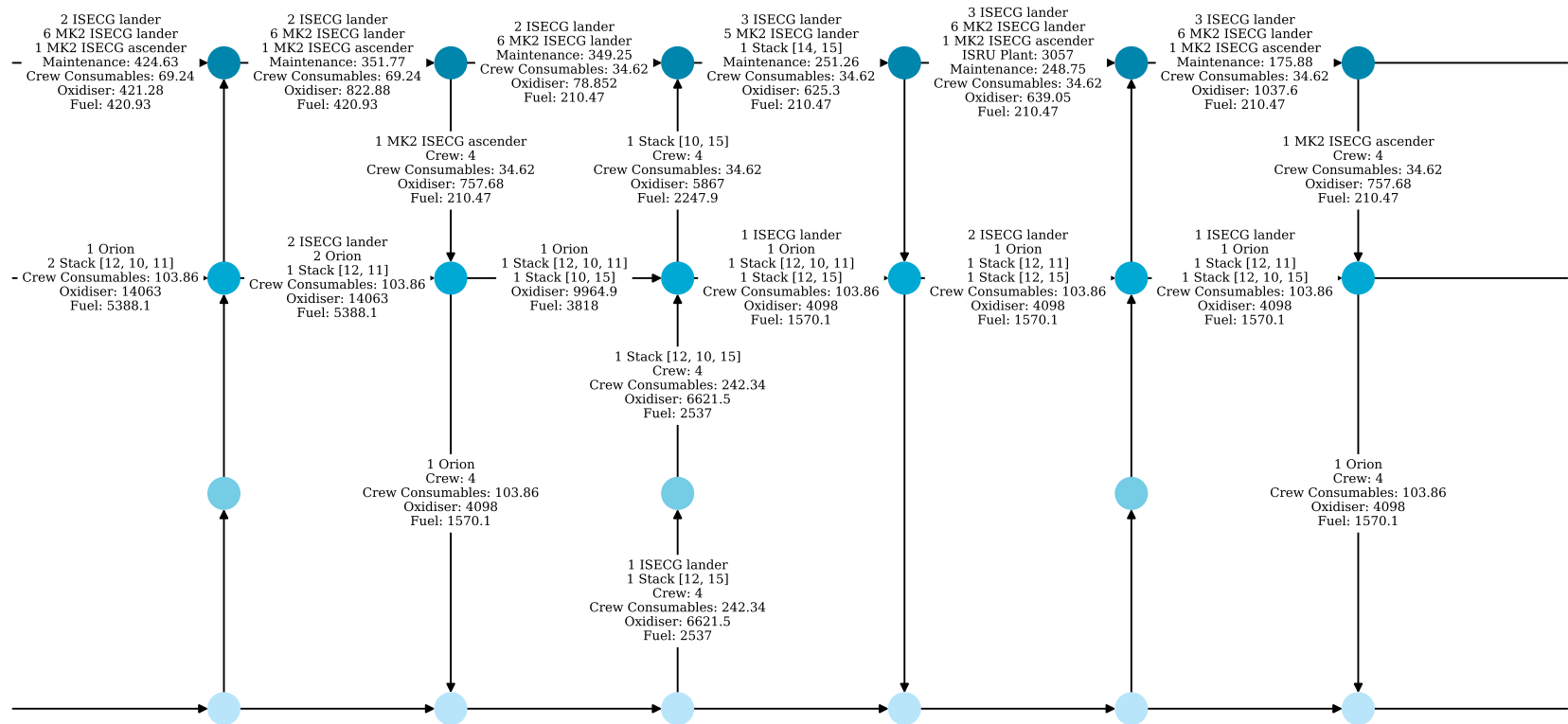


Fig. 10 (continued on next page).

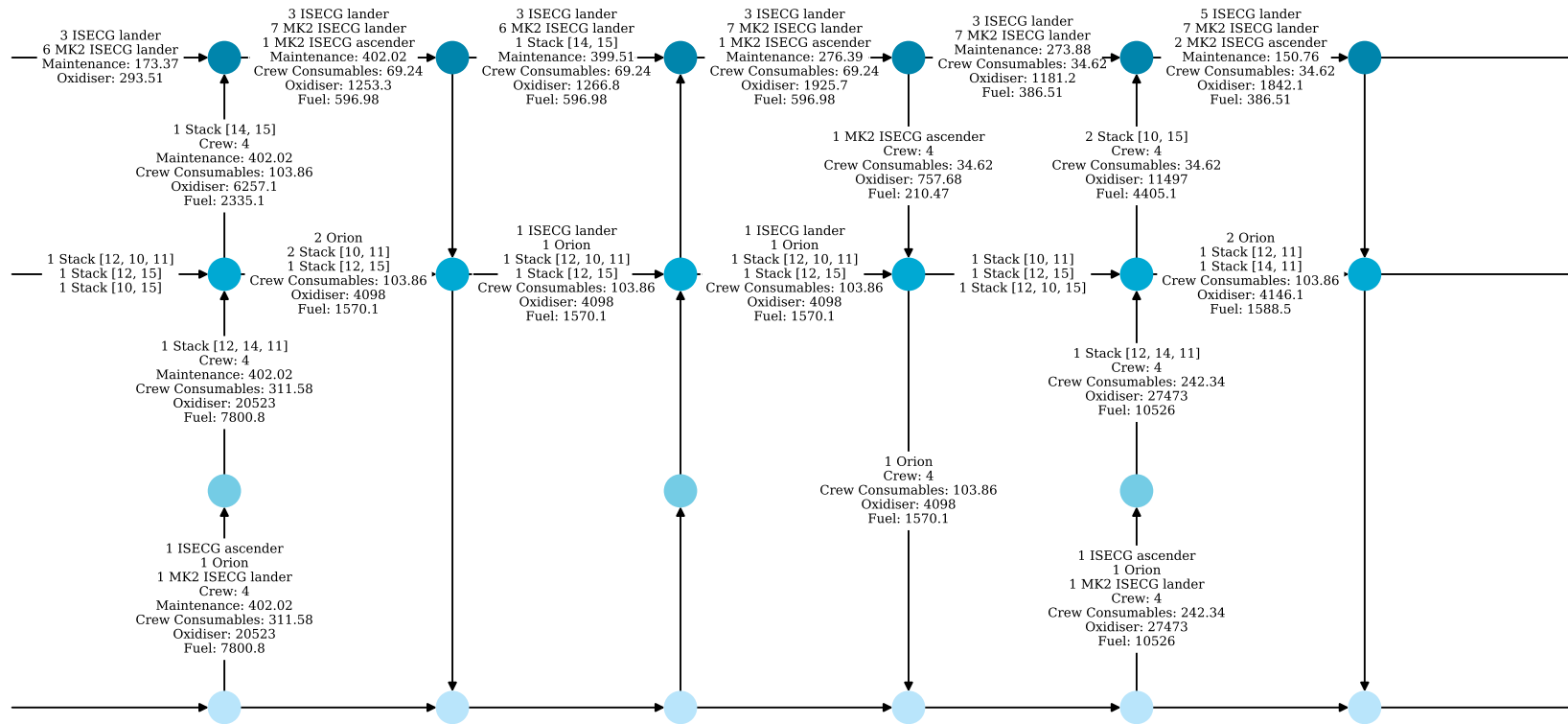


Fig. 10 (continued on next page).

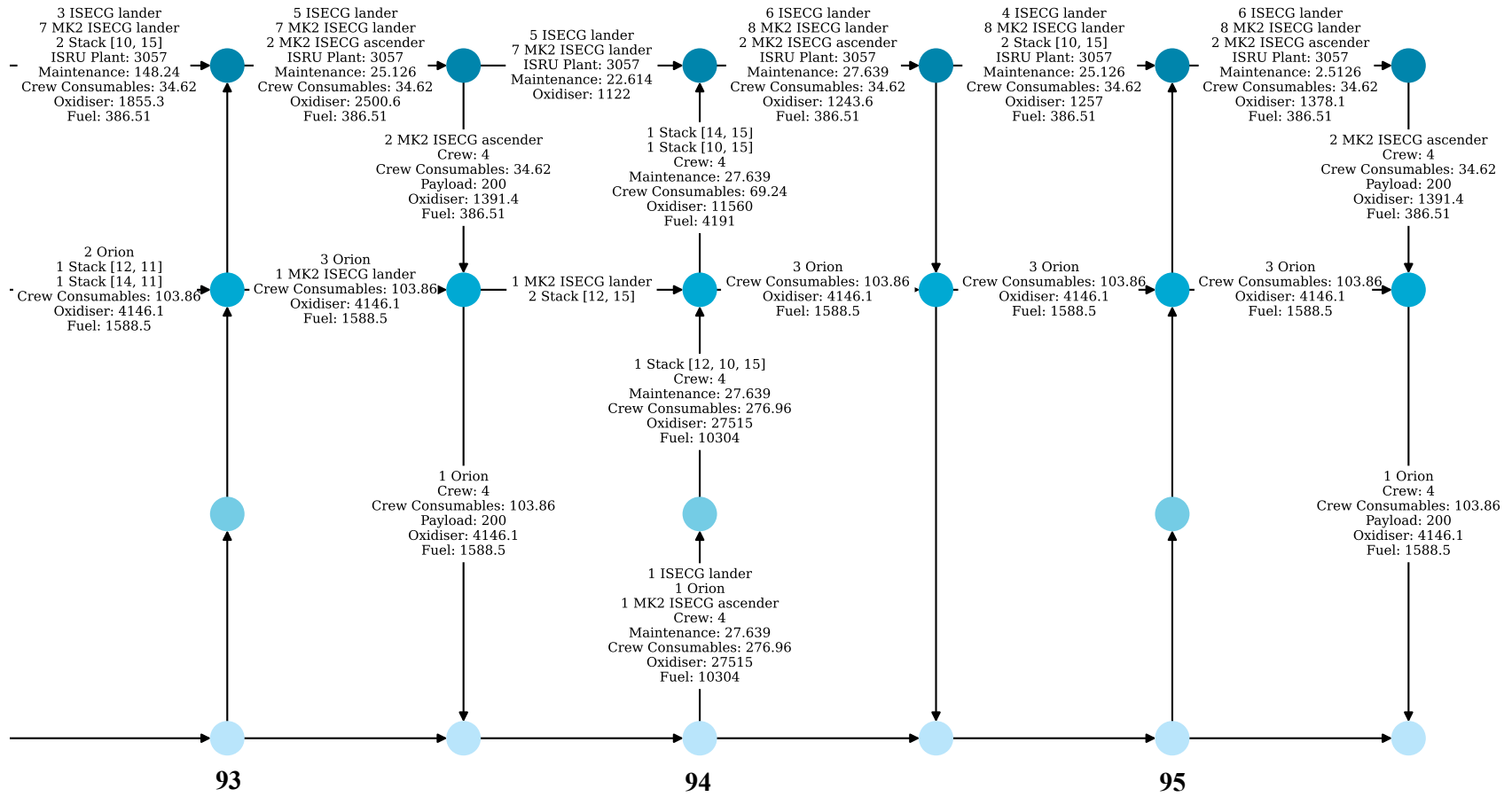
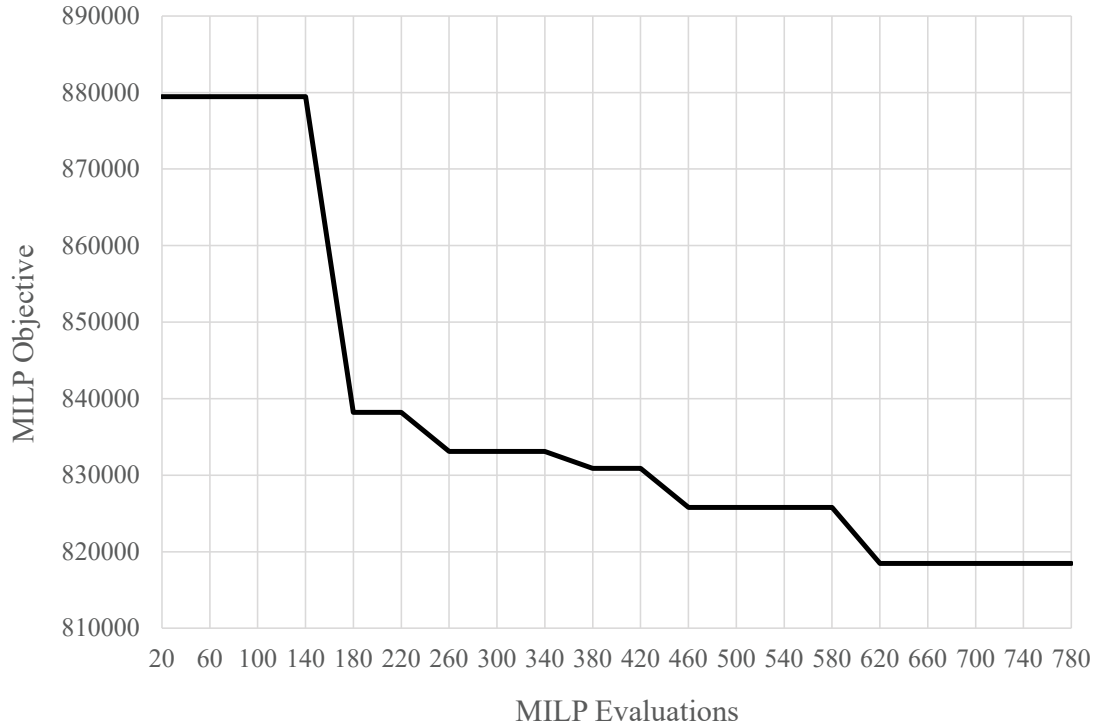


Fig. 10 Artemis phase 2B ConOps with improved schedule and optimized commodity flow.



**Fig. 11 Evolution of the objective of the Artemis Phase 2B model.**

As expected, it can be seen that the commodity flow optimizer ships ISRU infrastructure and maintenance supplies with the first mission of the campaign. In this particular solution, ISRU infrastructure is packed into the excess payload capability of logistics vehicles that are traveling with campaign payloads already. Therefore, the exact amount of ISRU infrastructure delivered to the lunar surface is dependent on the payload capability of the vehicles. Uncertainties in the logistics vehicle performance, such as engine  $I_{sp}$  or structure mass ratio, would propagate through to variation in available ISRU infrastructure, and therefore creating uncertainty in surface propellant availability. Further maintenance supplies are shipped with later missions. The inclusion of ISRU infrastructure prompts the scheduler to place the later missions later in their allowed windows, so that more propellant can be produced *in-situ* and reduce the amount required to be launched from Earth. For comparison, with ISRU capability disabled, the same solution produces an objective value of 845510 kg, demonstrating the net impact of ISRU on the logistics of the Artemis 2B scenario.

#### IV. Conclusion

This paper has presented a method for finding feasible exploration campaign plans subject to programmatic requirements, and in particular finding schedules that produce optimal commodity flow such that total launch mass across the entire campaign is minimized. By using a mixed-integer linear program to solve the optimal commodity flow for a given campaign plan, a genetic algorithm can then be used to find improved schedules with potentially nonlinear

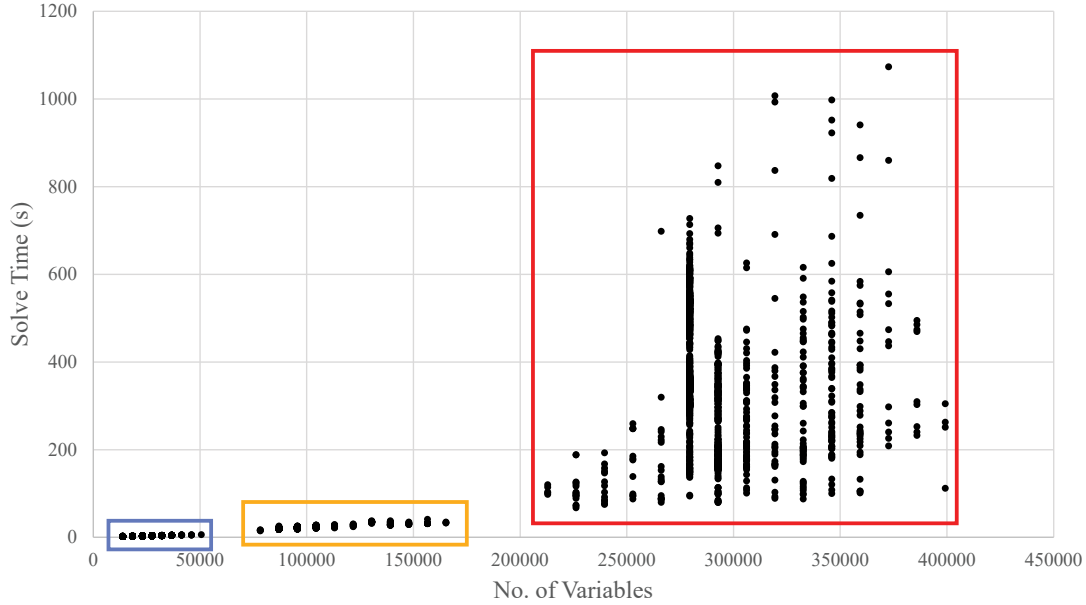


**Fig. 12** Solve times of the MILP versus the model size, measured across the CLPS (blue), Artemis Phase 1 - 2A (orange), and Artemis Phase 2B (red) case studies.

weighting. The scheduling algorithm was demonstrated with various example cases. In the case studies, it was found that medium-to-large class lunar landers are most effective in optimizing lunar exploration logistics and, in cases of low availability of those landers, smaller and readily available landers provide useful, though sub-optimal, alternatives.

### Appendix A: MILP Solver Performance

The commodity flow problem solve time was measured for each function evaluation of the case studies discussed in this paper. Figure 12 plots the solve time versus the number of variables present in each model. 5 islands in parallel of CLPS and Artemis Phase 1 - 2A models were solved using a PC with an 8-core Intel Core i7-10700 2.90GHz CPU and 32 GB RAM, and 2 islands in parallel of Artemis 2B models were solved using the Georgia Tech PACE cluster [61] with a 24-core Dual Intel Xeon Gold 6226 2.7 GHz CPU node and 32 GB RAM. The average solve time and the variance in the solve time increase exponentially with the model size. An all-in-MILP approach to the campaign scheduling problem would require a factor of  $\approx P \times T$  more variables than those the models tested in Figure 12, because it becomes necessary to index every payload in the campaign separately in order to formulate sequencing constraints, and it also becomes impossible to trim the MILP timeline to just the time stamps in the potential solution. The solve time for such a model would be unpredictable and likely extremely long. In addition, memory allocation issues would eventually be encountered. The method presented in this paper avoids this issue by repeatedly solving reduced commodity flow problems.

## Acknowledgment

The authors acknowledge Yuri Shimane and Masafumi Isaji for their helpful feedback and suggestions.

## References

- [1] International Space Exploration Coordination Group (ISECG), *Global Exploration Roadmap (GER) Supplement August 2020: Lunar Surface Exploration Scenario Update*, 2020. URL [https://www.globalspaceexploration.org/wp-content/uploads/2020/08/GER\\_2020\\_supplement.pdf](https://www.globalspaceexploration.org/wp-content/uploads/2020/08/GER_2020_supplement.pdf).
- [2] Fasano, G., “Mixed integer linear approach for the space station on-orbit resources re-supply,” *AIRO 96 Annual Conference Proceedings*, Perugia, Italy, 1996.
- [3] Fasano, G., and Provera, R., “A traffic model for the space station on-orbit re-supply problem,” *The International Society of Logistics Engineering (SOLE), Logistics National Conference Proceedings*, Turin, Italy, 1997.
- [4] Taylor, C., Klabjan, D., Simchi-levi, D., Song, M., and De Weck, O., “Modeling Interplanetary Logistics: A Mathematical Model for Mission Planning,” *AIAA Journal*, 2006. <https://doi.org/10.2514/6.2006-5735>.
- [5] Gralla, E., Shull, S., and de Weck, O., “A Modeling Framework for Interplanetary Supply Chains,” *Space 2006*, American Institute of Aeronautics and Astronautics, San Jose, California, 2006. <https://doi.org/10.2514/6.2006-7229>, URL <http://arc.aiaa.org/doi/10.2514/6.2006-7229>.
- [6] Grogan, P., Yue, H., and De Weck, O., “Space Logistics Modeling and Simulation Analysis using SpaceNet: Four Application Cases,” *AIAA SPACE 2011 Conference & Exposition*, American Institute of Aeronautics and Astronautics, Long Beach, California, 2011. <https://doi.org/10.2514/6.2011-7346>.
- [7] Ho, K., de Weck, O., Hoffman, J., and Shishko, R., “Dynamic modeling and optimization for space logistics using time-expanded networks,” *Acta Astronautica*, Vol. 105, 2014. <https://doi.org/10.1016/j.actaastro.2014.10.026>.
- [8] Ishimatsu, T., de Weck, O. L., Hoffman, J. A., Ohkami, Y., and Shishko, R., “Generalized Multicommodity Network Flow Model for the Earth–Moon–Mars Logistics System,” *Journal of Spacecraft and Rockets*, Vol. 53, No. 1, 2016, p. 25–38. <https://doi.org/10.2514/1.A33235>.
- [9] Chen, H., and Ho, K., “Integrated Space Logistics Mission Planning and Spacecraft Design with Mixed-Integer Nonlinear Programming,” *Journal of Spacecraft and Rockets*, Vol. 55, No. 2, 2018, p. 365–381. <https://doi.org/10.2514/1.A33905>.
- [10] Isaji, M., Takubo, Y., and Ho, K., “Multidisciplinary Design Optimization Approach to Integrated Space Mission Planning and Spacecraft Design,” *Journal of Spacecraft and Rockets*, Vol. 59, No. 5, 2021, p. 1660–1670. <https://doi.org/10.2514/1.A35284>.
- [11] Chen, H., Sarton du Jonchay, T., Hou, L., and Ho, K., “Multifidelity Space Mission Planning and Infrastructure Design Framework for Space Resource Logistics,” *Journal of Spacecraft and Rockets*, Vol. 58, No. 2, 2021, p. 538–551. <https://doi.org/10.2514/1.A34666>.

- [12] Takubo, Y., Chen, H., and Ho, K., “Hierarchical Reinforcement Learning Framework for Stochastic Spaceflight Campaign Design,” *Journal of Spacecraft and Rockets*, Vol. 59, No. 2, 2022, p. 421–433. <https://doi.org/10.2514/1.A35122>.
- [13] Blossey, G., “A Stochastic Modeling Approach for Interplanetary Supply Chain Planning,” *Space: Science & Technology*, Vol. 3, 2023, p. 0014. <https://doi.org/10.34133/space.0014>.
- [14] Chen, H., Gardner, B. M., Grogan, P. T., and Ho, K., “Flexibility Management for Space Logistics via Decision Rules,” *Journal of Spacecraft and Rockets*, Vol. 58, No. 5, 2021, p. 1314–1324. <https://doi.org/10.2514/1.A34985>.
- [15] Sarton du Jonchay, T., Chen, H., Gunasekara, O., and Ho, K., “Framework for modeling and optimization of on-orbit servicing operations under demand uncertainties,” *Journal of Spacecraft and Rockets*, Vol. 58, No. 4, 2021, pp. 1157–1173.
- [16] Goffin, J. L., Gondzio, J., Sarkissian, R., and Vial, J. P., “Solving nonlinear multicommodity flow problems by the analytic center cutting plane method,” *Mathematical Programming*, Vol. 76, No. 1, 1996, p. 131–154. <https://doi.org/10.1007/BF02614381>.
- [17] Castro, J., and Nabona, N., “An implementation of linear and nonlinear multicommodity network flows,” *European Journal of Operational Research*, Vol. 92, No. 1, 1996, p. 37–53. [https://doi.org/10.1016/0377-2217\(95\)00137-9](https://doi.org/10.1016/0377-2217(95)00137-9).
- [18] Mijangos, E., “Approximate Subgradient Methods for Nonlinearly Constrained Network Flow Problems,” *Journal of Optimization Theory and Applications*, Vol. 128, No. 1, 2006, p. 167–190. <https://doi.org/10.1007/s10957-005-7563-0>.
- [19] Alavidoost, M. H., Tarimoradi, M., and Zarandi, M. H. F., “Bi-objective mixed-integer nonlinear programming for multi-commodity tri-echelon supply chain networks,” *Journal of Intelligent Manufacturing*, Vol. 29, No. 4, 2018, p. 809–826. <https://doi.org/10.1007/s10845-015-1130-9>.
- [20] Jagannatha, B. B., and Ho, K., “Optimization of In-Space Supply Chain Design Using High-Thrust and Low-Thrust Propulsion Technologies,” *Journal of Spacecraft and Rockets*, Vol. 55, No. 3, 2018, p. 648–659. <https://doi.org/10.2514/1.A34042>.
- [21] Gollins, N. J., Isaji, M., Shimane, Y., and Ho, K., “A Heuristic Method for Determining Payload-to-Vehicle Assignment & Launch Order for Multi-Vehicle Exploration Campaigns,” *AIAA SCITECH 2023 Forum*, American Institute of Aeronautics and Astronautics, National Harbor, MD, 2023. <https://doi.org/10.2514/6.2023-1965>, URL <https://arc.aiaa.org/doi/10.2514/6.2023-1965>.
- [22] Jagannatha, B. B., and Ho, K., “Event-Driven Network Model for Space Mission Optimization with High-Thrust and Low-Thrust Spacecraft,” *Journal of Spacecraft and Rockets*, Vol. 57, No. 3, 2020, pp. 446–463. <https://doi.org/10.2514/1.A34628>.
- [23] Trent, D., “Integrated Architecture Analysis and Technology Evaluation for Systems of Systems Modeled at the Subsystem Level,” Ph.D. thesis, Georgia Institute of Technology, Atlanta, GA, Nov 2017. URL <https://repository.gatech.edu/entities/publication/79512a85-fe5f-4f18-9ef3-fbb29df593e>.
- [24] Edwards, S. J., Trent, D., Diaz, M. J., and Mavris, D. N., “A Model-Based Framework for Synthesis of Space Transportation Architectures,” *2018 AIAA SPACE and Astronautics Forum and Exposition*, American Institute of Aeronautics and Astronautics, Orlando, FL, 2018. <https://doi.org/10.2514/6.2018-5133>, URL <https://arc.aiaa.org/doi/10.2514/6.2018-5133>.

- [25] Downs, C., Prasad, A., Robertson, B. E., and Mavris, D. N., “A Spaceflight Logistics Approach to Modeling Novel Vehicle Concepts,” *AIAA SCITECH 2023 Forum*, American Institute of Aeronautics and Astronautics, National Harbor, MD & Online, 2023. <https://doi.org/10.2514/6.2023-1964>, URL <https://arc.aiaa.org/doi/10.2514/6.2023-1964>.
- [26] Morales, A. K., and Quezada, C. V., “C.V.: A universal eclectic genetic algorithm for constrained optimization,” *In: Proceedings 6th European Congress on Intelligent Techniques and Soft Computing*, Verlag, 1998, pp. 518–522.
- [27] Biscani, F., and Izzo, D., “A parallel global multiobjective framework for optimization: pagmo,” *Journal of Open Source Software*, Vol. 5, No. 53, 2020, p. 2338. <https://doi.org/10.21105/joss.02338>, URL <https://doi.org/10.21105/joss.02338>.
- [28] Parker, J. S., and Anderson, R. L., *Low-Energy Lunar Trajectory Design*, John Wiley & Sons, Inc., Hoboken, NJ, USA, 2014. <https://doi.org/10.1002/9781118855065>, URL <http://doi.wiley.com/10.1002/9781118855065>.
- [29] Gurobi Optimization, LLC, “Gurobi Optimizer Reference Manual,” , 2022. URL <https://www.gurobi.com>.
- [30] Hart, W. E., Watson, J.-P., and Woodruff, D. L., “Pyomo: modeling and solving mathematical programs in Python,” *Mathematical Programming Computation*, Vol. 3, No. 3, 2011, pp. 219–260.
- [31] Bynum, M. L., Hackebeil, G. A., Hart, W. E., Laird, C. D., Nicholson, B. L., Siirola, J. D., Watson, J.-P., and Woodruff, D. L., *Pyomo—optimization modeling in python*, 3<sup>rd</sup> ed., Vol. 67, Springer Science & Business Media, 2021.
- [32] Orloff, R. W., *Apollo by the numbers: a statistical reference*, NASA-SP, National Aeronautics and Space Administration, Washington, D.C, 2000.
- [33] Isaji, M., Maynard, I., and Chudoba, B., “A New Sizing Methodology for Lunar Surface Access Systems,” *AIAA Scitech 2020 Forum*, American Institute of Aeronautics and Astronautics, Orlando, FL, 2020. <https://doi.org/10.2514/6.2020-1775>, URL <https://arc.aiaa.org/doi/10.2514/6.2020-1775>.
- [34] Warner, C., “First Commercial Moon Delivery Assignments to Advance Artemis,” *NASA*, 2020. URL <http://www.nasa.gov/feature/first-commercial-moon-delivery-assignments-to-advance-artemis>, accessed: 2023-05-29.
- [35] Dunbar, B., “Commercial Lunar Payload Services Overview,” *NASA*, 2019. URL <http://www.nasa.gov/content/commercial-lunar-payload-services-overview>, accessed: 2022-11-18.
- [36] Vitug, E., “Polar Resources Ice Mining Experiment-1 (PRIME-1),” *NASA*, 2020. URL [http://www.nasa.gov/directorates/spacetech/game\\_changing\\_development/projects/PRIME-1](http://www.nasa.gov/directorates/spacetech/game_changing_development/projects/PRIME-1), accessed: 2022-11-18.
- [37] Colaprete, A., “A lunar water reconnaissance mission,” *NASA*, 2020, p. 25. URL <https://science.nasa.gov/science-pink/s3fs-public/atoms/files/09-Colaprete-VIPER%20Overview%20for%20PAC%2008172020.pdf>, accessed: 2022-11-18.
- [38] Potter, S., “NASA Selects Firefly Aerospace for Artemis Commercial Moon Delivery,” *NASA*, 2021. URL <http://www.nasa.gov/press-release/nasa-selects-firefly-aerospace-for-artemis-commercial-moon-delivery-in-2023>, accessed: 2022-11-18.

- [39] Dodson, G., “NASA Selects Draper to Fly Research to Far Side of Moon,” *NASA*, 2022. URL <http://www.nasa.gov/press-release/nasa-selects-draper-to-fly-research-to-far-side-of-moon>, accessed: 2022-11-18.
- [40] Astrobotic, “Astrobotic - Payload User Guide,” , 2019. URL <https://web.archive.org/web/20220907185216/https://www.astrobotic.com/wp-content/uploads/2021/01/Peregrine-Payload-Users-Guide.pdf>, accessed: 2022-11-18.
- [41] Astrobotic, “Astrobotic Lunar Landers Payload User’s Guide v.5,” , 2021. URL [https://www.astrobotic.com/wp-content/uploads/2022/01/PUGLanders\\_011222.pdf](https://www.astrobotic.com/wp-content/uploads/2022/01/PUGLanders_011222.pdf), accessed: 2022-11-18.
- [42] Astrobotic, “Griffin Lunar Test Model Complete,” , Feb 2022. URL <https://www.astrobotic.com/griffin-lunar-test-model-complete/>, accessed: 2022-11-18.
- [43] Blue Origin, “Blue Moon,” , 2022. URL <https://www.blueorigin.com/blue-moon>, accessed: 2022-11-16.
- [44] Blue Origin, “New Glenn Payload User’s Guide,” , 2018.
- [45] ispace, “Payload User’s Guide,” , 2020. URL [https://www.mach5lowdown.com/wp-content/uploads/PUG/ispace\\_PayladUserGuide\\_v2\\_202001.pdf](https://www.mach5lowdown.com/wp-content/uploads/PUG/ispace_PayladUserGuide_v2_202001.pdf).
- [46] ispace, “ispace Unveils Mission 3 Lander Design, Set to Launch in 2024,” , 2021. URL <https://ispace-inc.com/jpn/news/?p=2042>, accessed: 2022-11-18.
- [47] Firefly Aerospace, “Blue Ghost Lunar Lander Condensed Payload User’s Guide,” , 2021. URL [https://firefly.com/wp-content/uploads/2022/01/Blue\\_Ghost\\_PUG-1.pdf](https://firefly.com/wp-content/uploads/2022/01/Blue_Ghost_PUG-1.pdf).
- [48] Berger, E., “For lunar cargo delivery, NASA accepts risk in return for low prices,” *Ars Technica*, 2021. URL <https://arstechnica.com/science/2021/05/for-lunar-cargo-delivery-nasa-accepts-risk-in-return-for-low-prices/>, accessed: 2022-11-18.
- [49] Lockheed Martin, “McCandless Lunar Lander User’s Guide,” , 2019. URL [https://cdn2.hubspot.net/hubfs/517792/Space/McCandless\\_Lander\\_User\\_Guide\\_Release1.pdf](https://cdn2.hubspot.net/hubfs/517792/Space/McCandless_Lander_User_Guide_Release1.pdf), accessed: 2022-11-18.
- [50] Moon Express, “MX-1 Scout Class Explorer,” , Oct 2019. URL <https://web.archive.org/web/20191027184953/http://www.moonexpress.com/robotic-explorers/mx-1-scout-class-explorer/>, accessed: 2022-11-01.
- [51] Izzo, D., Ruciński, M., and Biscani, F., *The Generalized Island Model*, Springer Berlin Heidelberg, Berlin, Heidelberg, 2012, Studies in Computational Intelligence, Vol. 415, p. 151–169. [https://doi.org/10.1007/978-3-642-28789-3\\_7](https://doi.org/10.1007/978-3-642-28789-3_7), URL [https://link.springer.com/10.1007/978-3-642-28789-3\\_7](https://link.springer.com/10.1007/978-3-642-28789-3_7).
- [52] Hoshino, T., Wakabayashi, S., Ohtake, M., Karouji, Y., Hayashi, T., Morimoto, H., Shiraishi, H., Shimada, T., Hashimoto, T., Inoue, H., Hirasawa, R., Shirasawa, Y., Mizuno, H., and Kanamori, H., “Lunar polar exploration mission for water prospection - JAXA’s current status of joint study with ISRO,” *Acta Astronautica*, Vol. 176, 2020, p. 52–58. <https://doi.org/10.1016/j.actaastro.2020.05.054>.

- [53] Morisset, C.-E., Picard, M., and Moroso, F., “The Canadian Lunar Exploration Accelerator Program (LEAP) Rover Mission (LRM): Rove, Gather, Overcome, and Inspire.” *53rd Lunar and Planetary Science Conference*, Texas, USA, 2022.
- [54] Landgraf, M., Duvet, L., Cropp, A., Alvarez, G., Ambroszkiewicz, G., Bottacini, M., Brunner, P., Bucci, L., Carey, W., Casini, A. E. M., Cifani, G., Dubois-Matra, O., Ellwood, J., Gonzalez Fernandez, A., Gernoth, A., Getimis, A., Gonzalez Gomez, G., Greuel, D., Hager, P., Heindel, S., Lanucara, M., Le Deuff, Y., Mangunsong, S., Murray, N. P., Nardi, C.-V., Nasca, R., Nergaard, K., Nzokira, G., Renk, F., Rovelli, D., Schlutz, J., Schonenborg, R., Stephenson, K., Tavoularis, A., Termtanasombat, N., Thirkettle, A., Ventura, S., Sanchez de la Villa, B., Wohlhuter, M., and Magistrati, G., “Autonomous Access to the Moon for Europe: The European Large Logistic Lander,” *73rd International Astronautical Congress*, Paris, France, 2022.
- [55] Guidi, J., Haese, M., Landgraf, M., Lange, C., Pirrotta, S., and Sato, N., “The 2022 Updated Lunar Exploration Scenario for the Global Exploration Roadmap (GER): The Growing Global Effort and Momentum Going Forward to the Moon and Mars,” *73rd International Astronautical Congress*, Paris, France, 2022.
- [56] Biesbroek, R., *CDF STUDY REPORT: MOON VILLAGE - Conceptual Design of a Lunar Habitat*, 2020. URL [https://www.lpi.usra.edu/lunar/strategies/ESA-ESTEC\\_2020\\_MoonVillageLunarHabitatStudy.pdf](https://www.lpi.usra.edu/lunar/strategies/ESA-ESTEC_2020_MoonVillageLunarHabitatStudy.pdf).
- [57] Schreiner, S. S., Sibille, L., Dominguez, J. A., and Hoffman, J. A., “A parametric sizing model for Molten Regolith Electrolysis reactors to produce oxygen on the Moon,” *Advances in Space Research*, Vol. 57, No. 7, 2016, p. 1585–1603. <https://doi.org/10.1016/j.asr.2016.01.006>.
- [58] Gibson, M. A., Mason, L. S., Bowman, C. L., Poston, D. I., McClure, P. R., Creasy, J., and Robinson, C., “Development of NASA’s Small Fission Power System for Science and Human Exploration,” 2015.
- [59] Landgraf, M., “Pathways to Sustainability in Lunar Exploration Architectures,” *Journal of Spacecraft and Rockets*, Vol. 58, No. 6, 2021, p. 1681–1693. <https://doi.org/10.2514/1.A35019>.
- [60] NASA, *Space Launch System Lift Capabilities*, 2020. URL [https://www.nasa.gov/sites/default/files/atoms/files/sls\\_lift\\_capabilities\\_and\\_configurations\\_508\\_08202018\\_0.pdf](https://www.nasa.gov/sites/default/files/atoms/files/sls_lift_capabilities_and_configurations_508_08202018_0.pdf).
- [61] PACE, *Partnership for an Advanced Computing Environment (PACE)*, 2017. URL <http://www.pace.gatech.edu>.